

**Ruprecht-Karls-Universität Heidelberg**  
**Fakultät für Mathematik und Informatik**

**Masterarbeit**

**A FAMILY OF REPRESENTATIONS FOR  
THE MODULAR GROUP**

Name: Fabian Kißler  
Matrikelnummer: 3222997  
E-Mail-Adresse: fkissler@gmail.com  
Betreuer: Prof. Dr. Anna Wienhard  
Datum der Abgabe:

## Erklärung

Ich versichere, dass ich diese Masterarbeit selbstständig verfasst und nur die angegebenen Quellen und Hilfsmittel verwendet habe.

Heidelberg, .....

Datum

.....

Unterschrift

## Abstract

Marked boxes are configurations of points and lines in the real projective plane that comprise the initial data for Pappus' Theorem. Using Pappus' Theorem, Richard Schwartz defines a group of box operations  $G$  that acts on the set of marked boxes. Based on Schwartz' article "Pappus's Theorem and the Modular Group", we prove in detail that  $G$  is isomorphic to the modular group  $M$ , and that there is a faithful representation of  $M$  into the group of projective symmetries  $\mathcal{G}$ . Additionally, we investigate the fractal structure of Pappus Curves, which are topological circles associated with  $G$ -orbits of convex marked boxes, and numerically estimate their box dimension.

## Zusammenfassung

Marked Boxes sind Konfigurationen aus Punkten und Geraden in der reellen projektiven Ebene, welche die Ausgangsdaten für den Satz von Pappus beinhalten. Richard Schwartz definiert, mit Hilfe des Satzes von Pappus, eine Gruppe von Boxoperationen  $G$ , die auf der Menge von Marked Boxes wirkt. Basierend auf Schwartz' Artikel "Pappus's Theorem and the Modular Group", beweisen wir detailliert, dass  $G$  isomorph zur Modularen Gruppe  $M$  ist und, dass es eine treue Darstellung von  $M$  in die Gruppe der projektiven Symmetrien  $\mathcal{G}$  gibt. Zusätzlich untersuchen wir die fraktale Struktur von Pappus-Kurven - diese sind topologische Kreise, die mit  $G$ -Orbits konvexer Marked Boxes in Zusammenhang stehen - und schätzen numerisch deren Box-Dimension.

*Für Anne*

# Contents

<b>1</b>	<b>Introduction</b>	<b>1</b>
1.1	Motivation and Goals . . . . .	1
1.2	Structure of the Thesis . . . . .	2
<b>2</b>	<b>Background</b>	<b>4</b>
2.1	Projective Geometry . . . . .	4
2.2	Hyperbolic Geometry . . . . .	13
<b>3</b>	<b>Iterating Pappus' Theorem</b>	<b>15</b>
3.1	Convex Marked Boxes . . . . .	15
3.2	Box Operations . . . . .	17
3.3	Marked Boxes and Projective Symmetries . . . . .	24
<b>4</b>	<b>Pappus Curves</b>	<b>32</b>
4.1	Self-Similarity . . . . .	34
4.2	Box Dimension . . . . .	36

# 1 Introduction

## 1.1 Motivation and Goals

In his article “Pappus’s Theorem and the Modular Group” [7], Richard Schwartz makes Pappus’ Theorem (see Theorem 1.1) new again by “treating it as a dynamical system” on the set of so-called marked boxes.

Let  $\mathbb{RP}^2$  be the real projective plane.

**Theorem 1.1** (Proposition 5.3 in [4]). *Let  $l$  and  $l'$  be two distinct lines in  $\mathbb{RP}^2$ . Let  $A, B, C$  be three distinct points on  $l$ , different from  $X = l \cap l'$ . Let  $A', B', C'$  be three distinct points on  $l'$ , different from  $X$ . Define*

$$A'' = \overline{AB'} \cap \overline{A'B}, \quad B'' = \overline{AC'} \cap \overline{A'C}, \quad C'' = \overline{BC'} \cap \overline{B'C}.$$

*Then  $A'', B'',$  and  $C''$  are collinear.*

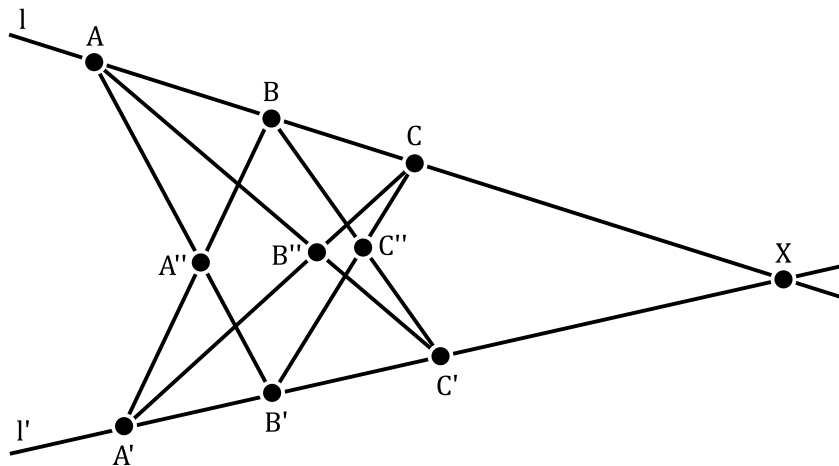


**Figure 1:** Pappus configuration.

Marked boxes comprise the initial data for Pappus’ Theorem. Here, they are given by the above-mentioned six points  $A, B, C, A', B',$  and  $C'$ . Given this input data, Pappus’ Theorem produces the points  $A'', B'',$  and  $C''$ . Schwartz observed that it is possible to iterate Pappus’ Theorem by combining the theorem’s input and its output to generate new initial data (and thus new marked boxes), i.e., the points  $A, B, C, A'', B'', C''$ , as well as  $A'', B'', C'', A', B', C'$  again represent suitable input for Pappus’ Theorem. This way, Schwartz introduces a group of box operations  $G$ , where each operation represents a way to generate new input data from given input data. Schwartz remarks that  $G$  is isomorphic to the modular group  $M$ .

Let  $\mathcal{G}$  be the group of projective symmetries of  $\mathbb{RP}^2$  (it is generated by projective transformations and dualities of  $\mathbb{RP}^2$ ). Besides the action of  $G$ , there is an action of  $\mathcal{G}$  on the set of marked boxes. Let  $\Theta$  be a marked box and let  $\Omega = G(\Theta)$  be its orbit under the action of  $G$ . Schwartz shows that there is a representation  $\overline{M}: M \rightarrow \mathcal{G}$  such that the image of  $\overline{M}$  is a group of projective symmetries of  $\Omega$ . If  $\Theta$  is convex, which is a geometric property of marked boxes, it can be shown that  $\overline{M}$  is faithful.

In the convex case, certain distinguished points of marked boxes in  $\Omega$  are dense in a topological circle, a so-called Pappus Curve, in  $\mathbb{RP}^2$ . Visualizing these curves, we notice that they exhibit lots of sharp bends and detail on small scales, which are characteristics of fractal sets.

The aims of this thesis are as follows:

1. Our first goal is to prove that the group of box operations  $G$  has the presentation  $\langle \alpha, \beta \mid \alpha^2, \beta^3 \rangle$ , which implies that it is isomorphic to the modular group.
2. We specify the matrices that represent the generators of the image of the representation  $\overline{M}: M \rightarrow \mathcal{G}$ , and show in detail that  $\overline{M}$  is faithful provided that  $\Theta$  is convex.
3. We verify that Pappus Curves have characteristics of fractal sets, like self-similarity. Additionally, we numerically estimate the box dimension of a family of Pappus Curves.

## 1.2 Structure of the Thesis

First, in Section 2.1, we introduce projective spaces as the projective closure of affine spaces and present models for the real projective line and plane. Based on this pictorial introduction, we give an analytical description of projective spaces and the corresponding dual spaces by introducing coordinates. This enables us to study symmetries of projective spaces, i.e., transformations that preserve incidence relations. The use of coordinates also facilitates the computation of cross-ratios, which determine the relative position of four points on a line, or the relative position of four lines in a pencil of lines. These results help us to understand the geometry of marked boxes in Section 3.

In Section 2.2 we define the modular group  $M$  as a group of hyperbolic isometries that is generated by two rotations. We observe that  $M$  acts as a group of graph isomorphisms on the graph that corresponds to the tiling of the hyperbolic

plane associated with the group that is generated by reflections in the sides of an ideal triangle. This result facilitates the proof of the main theorem of Section 3.3.

In Section 3.1 we introduce the set of convex marked boxes. The geometric notion of convexity allows for the proofs of the main theorems of Sections 3.2 and 3.3.

The objective of Section 3.2 is to prove that the group of box operations  $G$  is isomorphic to the modular group. To this end, we show that the action of  $G$  preserves convexity, i.e., every marked box in the orbit of a convex marked box under the action of  $G$  is convex.

The action of the group of projective symmetries  $\mathcal{G}$  on the set of marked boxes also preserves convexity and commutes with the action of  $G$ . The goal of Section 3.3 is to give a detailed proof of the existence of a faithful representation  $\bar{M}: M \rightarrow \mathcal{G}$  of the modular group into the group of projective symmetries. Furthermore, we show that the modular group acts as a group of projective symmetries on the  $G$ -orbits of convex marked boxes.

In Section 4 we investigate the fractal structure of Pappus Curves. We show that these curves have four properties that, according to Falconer [2], are typical for fractal sets: They are defined recursively; they have a fine and detailed structure that is difficult to describe; they are self-similar (see Section 4.1); and their box dimension is greater than their topological dimension (see Section 4.2). We numerically estimate the box dimension of a family of marked boxes by means of a box-counting algorithm.



## 2 Background

### 2.1 Projective Geometry

In this section we introduce basic definitions and theorems from projective geometry. Most of them can be found in Gerd Fischer's book "Analytische Geometrie" [3].

#### 2.1.1 Geometric Approach to Projective Spaces

Let  $Y_1$  and  $Y_2$  be lines in the Euclidean plane as shown in Figure 2. The central projection from  $Y_1$  to  $Y_2$  through the point  $z$  (which does not lie on either line) is defined as follows: The image of a point  $p \in Y_1$  is the point of intersection of the lines  $\overline{zp}$  and  $Y_2$ .

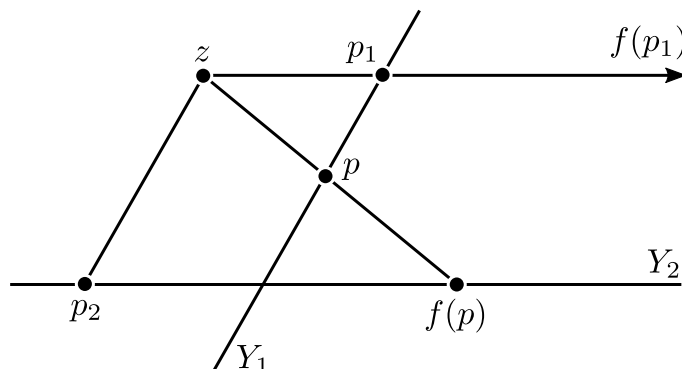


**Figure 2:** Central projection from  $Y_1$  to  $Y_2$  [3].

There is one point on  $Y_1$  that does not have an image and one point on  $Y_2$  that does not have a preimage. The point without image is  $p_1$  (the point of intersection of  $Y_1$  and the line that passes through  $z$  and is parallel to  $Y_2$ ). The point without preimage is  $p_2$  (the point of intersection of  $Y_2$  and the line that passes through  $z$  and is parallel to  $Y_1$ ). Hence, the above-defined central projection induces a bijective map

$$f: Y_1 \setminus \{p_1\} \rightarrow Y_2 \setminus \{p_2\}.$$

Now, consider a sequence of points  $(q_n)_{n \in \mathbb{N}} \subset Y_1 \setminus \{p_1\}$  that converges to  $p_1$ . In the corresponding sequence of image points  $(f(q_n))_{n \in \mathbb{N}} \subset Y_2$  we consequently find a subsequence that tends to plus or minus infinity on the line  $Y_2$ . However, we can make the sequence of image points converge if we add a single point at infinity  $\infty_2$  to  $Y_2$  and define this point as the limit of any sequence in  $Y_2$  that tends to plus or minus infinity. We call  $\overline{Y_2} = Y_2 \cup \{\infty_2\}$  the projective closure of  $Y_2$ . Similarly,

we define  $\overline{Y}_1 = Y_1 \cup \{\infty_1\}$ . We extend the projection  $f$  as follows:

$$\overline{f}: \overline{Y}_1 \rightarrow \overline{Y}_2,$$

with  $\overline{f}(p) = f(p)$  if  $p \neq p_1$ ,  $\overline{f}(p_1) = \infty_2$ , and  $\overline{f}(\infty_1) = p_2$ .

By adding points at infinity we can construct the closure of any line in the Euclidean plane. The projective closure of the whole plane is constructed by identifying points at infinity that belong to parallel lines and add them to the plane (which, according to Fischer, reflects the idea that parallel lines meet at infinity). This procedure can be generalized to define the projective closure of any real affine space  $X$ .

**Definition.** A **point at infinity** of  $X$  is an equivalence class of parallel lines in  $X$ . We denote the set of all points at infinity of  $X$  by  $X_\infty$  and we call

$$\overline{X} = X \cup X_\infty$$

the **projective closure** of  $X$ .

The projective closure of the affine spaces  $\mathbb{R}$  and  $\mathbb{R}^2$  are the real projective line  $\mathbb{RP}^1$  and the real projective plane  $\mathbb{RP}^2$ . In the following examples, we investigate the topology of these spaces.

**Example 2.1.** In  $\mathbb{R}$  there is just a single line, namely,  $\mathbb{R}$  itself. Hence, there is only one point at infinity and the projective closure is

$$\overline{\mathbb{R}} = \mathbb{R} \cup \{\infty\}.$$

As shown in Figure 3, using a stereographic projection through the north pole  $N$  of the circle  $\mathbb{S}^1$ , we get a bijective map  $\iota: \mathbb{R} \rightarrow \mathbb{S}^1 \setminus \{N\}$ . If we furthermore identify the point at infinity with the circle's north pole, we naturally get a bijective map from  $\mathbb{RP}^1$  onto  $\mathbb{S}^1$ .

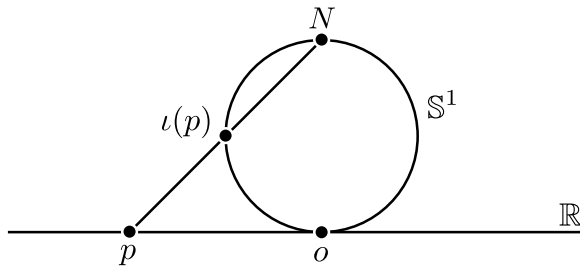


**Figure 3:** Projective closure of the real affine line [3].

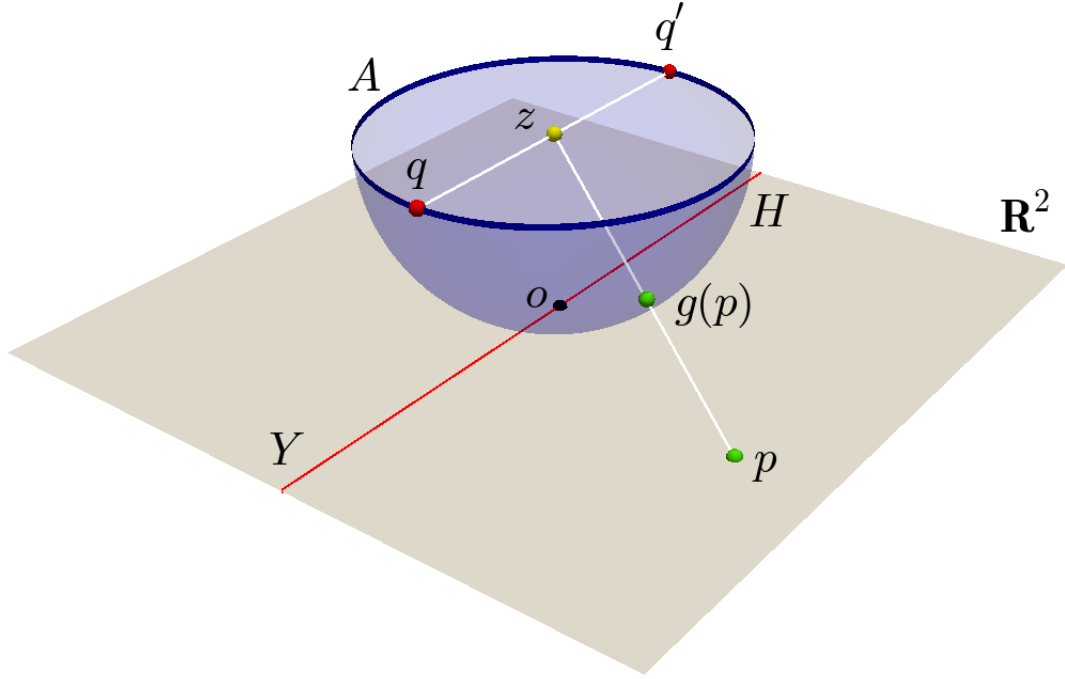


**Figure 4:** Projective closure of the real affine plane [3].

**Example 2.2.** To construct a model for  $\mathbb{RP}^2$ , we first identify  $\mathbb{R}^2$  with an open hemisphere  $H$  (see Figure 4) using a projection  $g: \mathbb{R}^2 \rightarrow H$  from the equator's midpoint  $z$ . Here, open means that the equator  $A$  is not a subset of  $H$ .

Every point at infinity  $p_\infty \in \mathbb{R}_\infty^2$  is represented by a unique line  $Y$  through the origin  $o$ . The line through  $z$  that is parallel to  $Y$  intersects the equator in a pair of antipodal points  $q$  and  $q'$ . By identifying antipodal points on the equator we obtain a quotient set  $A'$  and we get a natural bijection between  $A'$  and  $\mathbb{R}_\infty^2$ . As a result, we now have a bijection between  $\mathbb{RP}^2$  and  $H \cup A'$ .

The quotient set  $A'$  is homeomorphic to a circle  $\mathbb{S}^1$ . Since we identified  $\mathbb{R}_\infty^2$  with  $A'$  we can think of  $\mathbb{R}_\infty^2$  as a projective line (as in Example 2.1) at infinity.

**Example 2.3.** We find a second model for  $\mathbb{RP}^2$  by identifying antipodal points of the sphere  $\mathbb{S}^2$ . Thereby, we glue the upper and lower hemisphere of  $\mathbb{S}^2$  together and the points of the equator are identified in the same way as before. We get the natural quotient map

$$\rho: \mathbb{S}^2 \rightarrow \mathbb{RP}^2.$$

In this model, the points of  $\mathbb{RP}^2$  are pairs of antipodal points of  $\mathbb{S}^2$  and lines are represented by great circles on the sphere.

In Example 2.2, we constructed the projective closure of the Euclidean plane by adding points at infinity (equivalence classes of parallel lines) to  $\mathbb{R}^2$ . It turned out that the set of all points at infinity itself is a projective line, and if we remove this

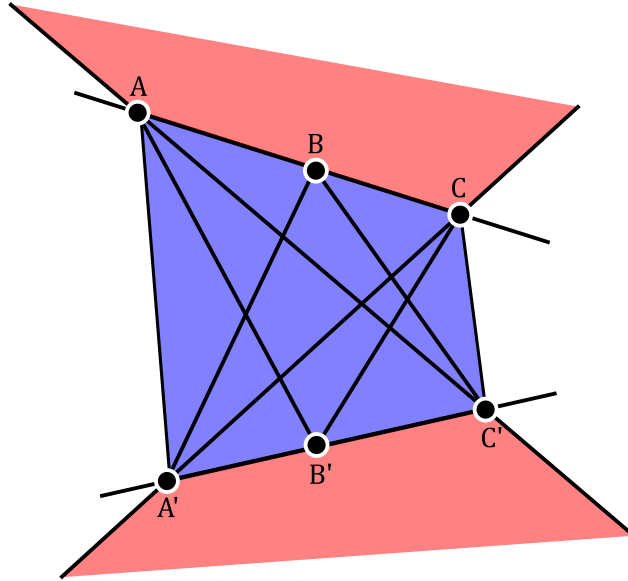


**Figure 5:** Pappus configuration and convex sets.

line from  $\mathbb{RP}^2$  we obtain the original affine space. However, Fischer remarks that from a projective point of view, it is not advisable to label a specific projective line as “the” line at infinity. He shows (see Theorem 3.2.2 in [3]) that for an arbitrary line  $Z \subset \mathbb{RP}^2$  we can equip the complement  $X = \mathbb{RP}^2 \setminus Z$  with the structure of an affine plane such that there is a canonical bijective map  $Z \rightarrow X_\infty$ , and  $Z$  can be regarded as the line at infinity of  $X$ .

This observation enables us to transfer the notion of convexity from the affine to the projective plane.

**Definition.** A subset  $C$  of the real projective plane  $\mathbb{RP}^2$  is **convex** if there is a line  $Z$  that does not intersect  $C$ , and  $C$  is convex in the affine space  $\mathbb{RP}^2 \setminus Z$ .

**Example 2.4.** In the Pappus configuration that is shown in Figure 5, the blue and the red quadrilateral, whose vertices, in cyclic order, are  $A, C, C', A'$ , and  $A', C', A, C$ , respectively, are convex.

With the definition of the projective closure of an affine space and the above-mentioned examples we developed first concepts of projective spaces, like the real projective line or plane. In addition to this geometrical way of thinking, in the following, we give an analytical introduction to projective spaces which directly enables us to define and study basic properties of projective transformations.

### 2.1.2 Analytical Approach to Projective Spaces

In Example 2.3, we introduced the sphere model for the projective plane, where the plane’s points correspond to pairs of antipodal points and its lines correspond

to great circles on the sphere. Imagine that this sphere is centered at the origin of the vector space  $\mathbb{R}^3$ . Every pair of antipodal points is the intersection of the sphere with a one-dimensional linear subspace of  $\mathbb{R}^3$ ; and every great circle is the intersection of the sphere with a two-dimensional linear subspace of  $\mathbb{R}^3$ . Hence, the points and lines of the real projective plane correspond to the one- and two-dimensional linear subspaces of  $\mathbb{R}^3$ .

We generalize this approach for projective spaces of arbitrary dimension.

**Definition.** Let  $V$  be a finite-dimensional real vector space.

- The **projective space**  $\mathbb{P}(V)$  is the set of one-dimensional linear subspaces of  $V$ . The **dimension** of  $\mathbb{P}(V)$  is  $\dim_{\mathbb{R}} \mathbb{P}(V) = \dim_{\mathbb{R}}(V) - 1$ .
- A subset  $Z \subset \mathbb{P}(V)$  is a **projective subspace** if the set  $U = \bigcup_{p \in Z} p$  is a linear subspace of  $V$ . The dimension of  $Z$  is  $\dim_{\mathbb{R}} Z = \dim_{\mathbb{R}}(U) - 1$ .

If  $V = \mathbb{R}^{n+1}$  we write  $\mathbb{R}\mathbb{P}^n = \mathbb{P}(\mathbb{R}^{n+1})$ .

**Definition.** In  $\mathbb{R}\mathbb{P}^n$ , using the standard basis  $(e_0, e_1, \dots, e_n)$  of  $\mathbb{R}^{n+1}$ , we can represent any line  $\mathbb{R}v$ , where  $v = (x_0, \dots, x_n)$  is a non-zero vector, by its **homogeneous coordinates**

$$(x_0 : x_1 : \dots : x_n) := \mathbb{R}v.$$

The linear forms  $(e_0^*, e_1^*, \dots, e_n^*)$ , that satisfy  $e_i^*(e_j) = \delta_{ij}$ , are a basis for the dual space  $(\mathbb{R}^{n+1})^*$ . Using this basis, every linear form has a unique representation  $\varphi = a_0 e_0^* + a_1 e_1^* + \dots + a_n e_n^*$ . If  $\varphi$  is non-zero then the line  $\mathbb{R}\varphi$  is an element of  $(\mathbb{R}\mathbb{P}^n)^* = \mathbb{P}((\mathbb{R}^{n+1})^*)$ , the projective dual space to  $\mathbb{R}\mathbb{P}^n$ , and we denote the homogeneous coordinates of  $\mathbb{R}\varphi$  by

$$(a_0 : a_1 : \dots : a_n) := \mathbb{R}\varphi.$$

The point  $\mathbb{R}\varphi$  corresponds to the hyperplane

$$H = \{(x_0 : x_1 : \dots : x_n) \in \mathbb{R}\mathbb{P}^n : a_0 x_0 + a_1 x_1 + \dots + a_n x_n = 0\}$$

and we call the tuple  $(a_0 : a_1 : \dots : a_n)$  the homogeneous coordinates of the hyperplane  $H$ . Thus, we can identify the dual space  $(\mathbb{R}\mathbb{P}^n)^*$  with the space of hyperplanes of  $\mathbb{R}\mathbb{P}^n$ .

**Definition.** A **pencil of hyperplanes**  $P$  in  $\mathbb{R}\mathbb{P}^n$  is a line in  $(\mathbb{R}\mathbb{P}^n)^*$ . Its **axis** is given by  $A = H_0 \cap H_1$  for two distinct hyperplanes  $H_0$  and  $H_1$  in  $P$ .

The dimension of an axis  $A$  of a pencil of hyperplanes is  $\dim_{\mathbb{R}} A = n - 2$ . In the real projective plane, a pencil of hyperplanes is called a pencil of lines. In this case, the axis  $A$  is a point and the pencil contains all the lines passing through  $A$ .

Next, we investigate maps between projective spaces.

### 2.1.3 Projective Symmetries

Let  $V$  and  $W$  be finite-dimensional real vector spaces.

**Definition.** A map  $f: \mathbb{P}(V) \rightarrow \mathbb{P}(W)$  is called a **projective transformation** if there is an isomorphism  $F: V \rightarrow W$  such that  $f(\mathbb{R}v) = \mathbb{R}F(v)$  for all  $v \in V \setminus \{0\}$ .

The choice of the linear isomorphism  $F$  is unique up to scaling with a non-zero real number. Linear isomorphisms map linear subspaces to linear subspaces. We conclude that projective transformations map projective subspaces to projective subspaces. In particular, projective transformations are collineations, i.e., they map collinear points to collinear points.

**Definition.** A **projective basis** of  $\mathbb{P}(V)$  is an  $(n + 2)$ -tuple  $(p_0, p_1, \dots, p_{n+1})$  of points such that no hyperplane contains  $n + 1$  of them.

**Example 2.5.** The four points  $A, C, C'$ , and  $A'$  of the Pappus configuration that is shown in Figure 1 are a projective basis of the real projective plane.

Projective transformations are determined by the image of a projective basis.

**Theorem 2.1** (Theorem 3.2.5 in [3]). *Let  $\mathbb{P}(V)$  and  $\mathbb{P}(W)$  be projective spaces of the same dimension with projective bases  $(p_0, p_1, \dots, p_{n+1})$  and  $(q_0, q_1, \dots, q_{n+1})$ . Then there is a unique projective transformation  $f: \mathbb{P}(V) \rightarrow \mathbb{P}(W)$  such that  $f(p_i) = q_i$  for all  $i = 0, 1, \dots, n + 1$ .*

**Definition.** A **projective coordinate system** for  $\mathbb{P}(V)$  is a projective transformation  $\kappa: \mathbb{R}\mathbb{P}^n \rightarrow \mathbb{P}(V)$ . If  $p = \kappa((x_0 : x_1 : \dots : x_n)) \in \mathbb{P}(V)$  then we call the vector  $(x_0 : x_1 : \dots : x_n)$  the **homogeneous coordinates of the point  $p$** .

The group of projective transformations of  $\mathbb{R}\mathbb{P}^n$  is the projective linear group  $PGL(n + 1, \mathbb{R})$ . Using projective coordinate systems, we can represent any projective transformation  $f: \mathbb{P}(V) \rightarrow \mathbb{P}(W)$  by an element of  $PGL(n + 1, \mathbb{R})$ , which is illustrated in the following commutative diagram:

$$\begin{array}{ccc} \mathbb{P}(V) & \xrightarrow{f} & \mathbb{P}(W) \\ \kappa \uparrow & & \downarrow (\kappa')^{-1} \\ \mathbb{R}\mathbb{P}^n & \xrightarrow{f'} & \mathbb{R}\mathbb{P}^n \end{array}$$

Projective transformations map projective subspaces to projective subspaces of the same dimension. If the subspace is a hyperplane, we can directly use its above-defined homogeneous coordinates to compute its image under such a transformation. Here are two technical lemmata that facilitate this computation:

Let  $\langle \cdot, \cdot \rangle$  be the standard inner product on  $\mathbb{R}^{n+1}$  and let  $H \subset \mathbb{RP}^n$  be a hyperplane with coordinate vector  $a = (a_0 : a_1 : \dots : a_n)$ . Let  $T$  be a matrix that represents a projective transformation of  $\mathbb{RP}^n$ .

**Lemma 2.2.** *The coordinate vector of the hyperplane  $T(H) \subset \mathbb{RP}^n$  is given by  $T^{-T}(a)$ .*

*Proof.* The image of  $H$  under the projective transformation  $T$  is a hyperplane in  $\mathbb{RP}^n$ . The preimage of an element  $y \in T(H)$  is a point in  $H$  and thus satisfies  $\langle a, T^{-1}(y) \rangle = 0$ , which is equivalent to  $\langle T^{-T}(a), y \rangle = 0$ .  $\square$

**Definition.** A **duality** is a projective transformation from  $\mathbb{RP}^n$  to  $(\mathbb{RP}^n)^*$ .

The image of a projective subspace  $Z \subset \mathbb{RP}^n$  under a duality  $\Delta$  is a projective subspace of  $(\mathbb{RP}^n)^*$  that can be identified with a subspace of  $\mathbb{RP}^n$  (similar to the above-mentioned identification of points and hyperplanes).

Let  $\Delta$  be a matrix that represents a duality and let  $H$  be the above-mentioned hyperplane.

**Lemma 2.3.** *The coordinate vector of the point  $\Delta(H) \in \mathbb{RP}^n$  is given by  $\Delta^{-T}(a)$ .*

*Proof.* The image of  $H$  under the duality  $\Delta$  is a hyperplane in the dual space  $(\mathbb{RP}^n)^*$ . The preimage of an element  $y \in \Delta(H)$  is a point in  $H$  and thus satisfies  $\langle a, \Delta^{-1}(y) \rangle = 0$ , which is equivalent to  $\langle \Delta^{-T}(a), y \rangle = 0$ .  $\square$

Let  $P(V)$  be the set of projective subspaces of  $\mathbb{P}(V)$ . We have seen that there is a natural action of projective transformations and dualities on  $P(V)$ .

**Definition.** A duality  $\Delta$  is called a **polarity** if  $\Delta(\Delta(Z)) = Z$  for all  $Z \in P(V)$ .

In  $\mathbb{RP}^2$  projective transformations map collinear points to collinear points (and thus, they map lines to lines). As illustrated in Figure 6, dualities map collinear points to a pencil of lines, and vice versa.

**Definition.** We call the group  $\mathcal{G}$  that is generated by projective transformations and dualities acting on  $P(\mathbb{R}^3)$  the group of **projective symmetries** of  $\mathbb{RP}^2$ .

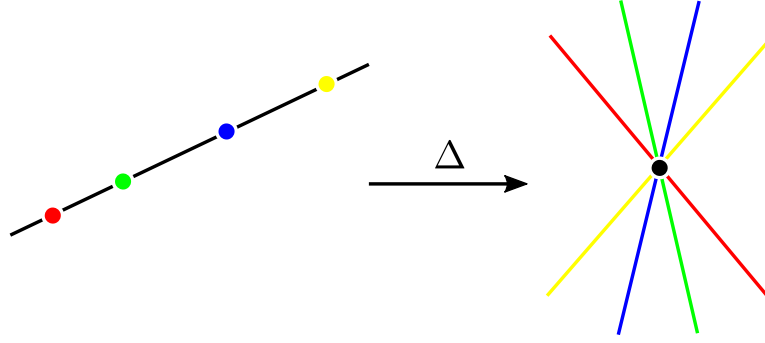


**Figure 6:** Dualities preserve incidence relations.

#### 2.1.4 Cross-Ratio

Let  $p_0, p_1, p_2$ , and  $p$  be collinear points in a projective space  $\mathbb{P}(V)$  such that  $p_0, p_1$ , and  $p_2$  are pairwise distinct and let  $Z$  be the line through these points. Then, the triple  $(p_0, p_1, p_2)$  is a projective basis for  $Z$ . Let  $\kappa: \mathbb{RP}^1 \rightarrow Z$  be a coordinate system for  $Z$  such that  $p_0 = \kappa((1 : 0))$ ,  $p_1 = \kappa((0 : 1))$ , and  $p_2 = \kappa((1 : 1))$ .

**Definition.** Let, using the above-defined projective basis for  $Z$ , the homogeneous coordinates of the point  $p$  be given by  $(\lambda : \mu) = \kappa^{-1}(p) \in \mathbb{RP}^1$ . We define the **cross-ratio** of the four points by

$$[p_0, p_1; p_2, p] := \lambda/\mu \in \mathbb{R} \cup \{\infty\}.$$

**Lemma 2.4** (Remark 3.3.1 in [3]). *The cross-ratio is invariant under projective transformations, i.e., for a projective transformation  $f: \mathbb{P}(V) \rightarrow \mathbb{P}(W)$  and the four points from the definition above, we have*

$$[p_0, p_1; p_2, p] = [f(p_0), f(p_1); f(p_2), f(p)].$$

In Figure 7, we use the circle model for the real projective line (see Example 2.1 and Figure 3) to illustrate the definition of the cross-ratio. Here, the point  $p$  is given the coordinates  $(1 : \frac{\mu}{\lambda})$  to emphasize that the cross-ratio can be interpreted as a parametrization of a projective line.

**Observation 2.5.** *We also observe that the cross-ratio of the four points (ordered as in the definition above) is negative if and only if  $p_0$  and  $p_1$  separate  $p_2$  and  $p$  on the line  $Z$ , as shown in Figure 7.*

Fischer presents a formula to facilitate the computation of the cross-ratio of a quadruple of points on a line  $Z \subset \mathbb{RP}^n$ .



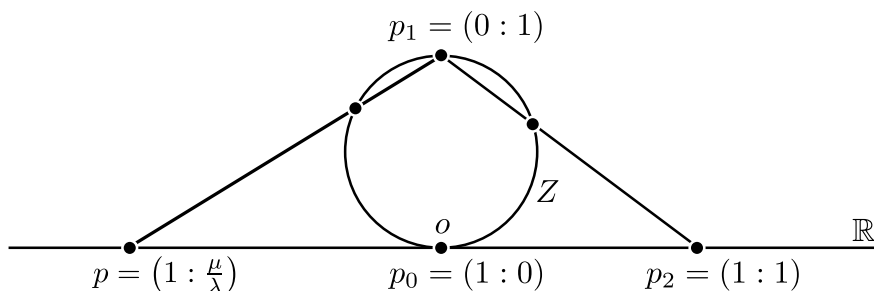


**Figure 7:** Cross-ratio of four points on a line.

**Lemma 2.6** (Lemma 3.3.2 in [3]). *Let  $p_k = (x_0^k : x_1^k : \dots : x_n^k)$  with  $k = 0, 1, 2, 3$  be four collinear points in  $\mathbb{RP}^n$  such that  $p_0, p_1$ , and  $p_2$  are pairwise distinct. If  $i, j \in \{0, 1, \dots, n\}$  are two distinct indices such that the points  $(x_i^0 : x_j^0)$ ,  $(x_i^1 : x_j^1)$ ,  $(x_i^2 : x_j^2) \in \mathbb{RP}^1$  are pairwise distinct, then*

$$[p_0, p_1; p_2, p] = \frac{\begin{vmatrix} x_i^3 & x_j^1 \\ x_j^3 & x_j^1 \end{vmatrix}}{\begin{vmatrix} x_i^3 & x_i^0 \\ x_j^3 & x_j^0 \end{vmatrix}} : \frac{\begin{vmatrix} x_i^2 & x_j^1 \\ x_j^2 & x_j^1 \end{vmatrix}}{\begin{vmatrix} x_i^2 & x_i^0 \\ x_j^2 & x_j^0 \end{vmatrix}}.$$

Let  $H_0, H_1, H_2$ , and  $H$  be four hyperplanes in a common pencil in  $\mathbb{RP}^n$  with axis  $A$  such that  $H_0, H_1$ , and  $H_2$  are pairwise distinct. A pencil of hyperplanes is a line in  $(\mathbb{RP}^n)^*$ , where hyperplanes are represented as points on that line. This allows for the definition of the cross-ratio of hyperplanes  $[H_0, H_1; H_2, H]$ . We can compute this ratio with the formula given in Lemma 2.6.

**Lemma 2.7** (Lemma 3.4.8 in [3]). *Let  $H_0, H_1, H_2$ , and  $H$  be hyperplanes in the above-mentioned pencil with axis  $A$ . Let  $Z$  be a line in  $\mathbb{RP}^n$  such that  $\mathbb{RP}^n$  is the smallest projective subspace that contains the line  $Z$  and the axis  $A$ . Define  $p_0 = Z \cap H_0$ ,  $p_1 = Z \cap H_1$ ,  $p_2 = Z \cap H_2$ , and  $p = Z \cap H$ . Then*

$$[H_0, H_1; H_2, H] = [p_0, p_1; p_2, p].$$

Figure 8 shows four lines  $H_0, H_1, H_2$ , and  $H_3$  in the projective plane in a pencil through the point  $A$ , a line  $Z$  that does not pass through  $A$ , and the points of intersection  $p_i$  of  $Z$  with the lines  $H_i$ .

**Observation 2.8.** *The lines  $H_0$  and  $H_1$  separate  $H_2$  and  $H_3$  in the pencil of lines through the point  $A$ , in the cyclic ordering of lines through  $A$  if and only if the points  $p_0$  and  $p_1$  separate  $p_2$  and  $p_3$  on the line  $Z$ .*

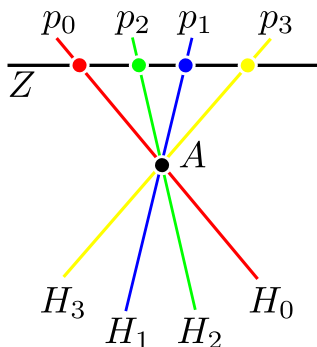


**Figure 8:** Illustration of Lemma 2.7 in the projective plane.

Combining Observation 2.5 and Lemma 2.7, now, we are able to determine the relative position of four lines in a pencil of lines in the projective plane only by computing their cross-ratio.

**Observation 2.9.** *The lines  $H_0$  and  $H_1$  separate  $H_2$  and  $H_3$  in the pencil of lines through the point  $A$ , in the cyclic ordering of lines through  $A$  if and only if the cross-ratio  $[H_0, H_1; H_2, H_3]$  is negative.*

## 2.2 Hyperbolic Geometry

Let  $\mathbb{C}$  be the complex plane. The following definition is from Svetlana Katok’s book “Fuchsian Groups” [6].

**Definition.** The **Poincaré disc model** of hyperbolic geometry is the unit disc  $D = \{z \in \mathbb{C} : |z| < 1\}$  equipped with the metric derived from the differential

$$ds = \frac{2|dz|}{1 - |z|^2}.$$

The boundary of the disc is the circle  $\partial D = \{z \in \mathbb{C} : |z| = 1\}$ . In the Poincaré disc model geodesics are segments of Euclidean circles orthogonal to the boundary  $\partial D$  and its diameters.

Figure 9 illustrates a finite portion of the tiling of the hyperbolic plane associated with the group that is generated by reflections in the sides of an ideal triangle. The edges of the triangles in the tiling together with their vertices form an undirected graph  $\Gamma$ .

**Definition.** The **modular group**  $M$  is a group of isometries of the hyperbolic plane. It is generated by an order two isometric rotation  $R_2$  about the center of the edge  $c$  (blue dot in Figure 9) and an order three isometric rotation  $R_3$  about the center of the ideal triangle bounded by the edges  $a$ ,  $b$ , and  $c$  (red dot in Figure 9).

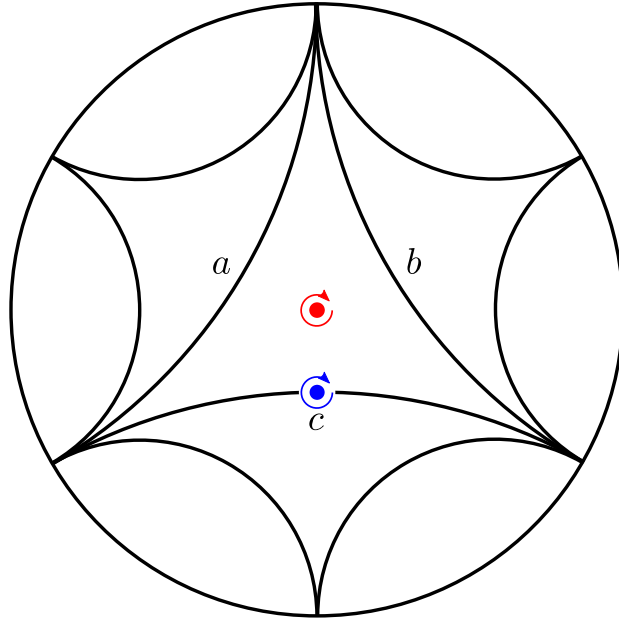


**Figure 9:** Poincaré disc model of the hyperbolic plane with geodesics.

Roger Alperin [1] shows that the modular group is isomorphic to the free product of cyclic groups  $Z_2 * Z_3$ . Thus,  $M$  has the presentation

$$M \cong \langle \alpha, \beta \mid \alpha^2, \beta^3 \rangle.$$

From the definition of the modular group, it follows that it naturally acts as a group of graph isomorphisms on the edges and vertices of  $\Gamma$ .

### 3 Iterating Pappus' Theorem

This section, including its structure, is based on Richard Schwartz' article "Pappus's Theorem and the Modular Group" [7].

#### 3.1 Convex Marked Boxes

**Definition.** An **overmarked box** is a pair of 6-tuples of points and lines in the projective plane

$$((p, q, r, s; t, b), (P, Q, R, S; T, B))$$

having the incidence relations as shown in Figure 10. The six points are pairwise distinct and different from the point  $T \cap B$ .

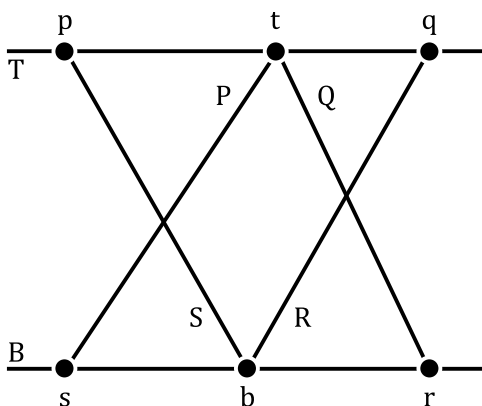


**Figure 10:** Incidence relations of points and lines that define an overmarked box [7].

There is an involution on the set of overmarked boxes that interchanges the points  $p$  and  $q$ , as well as  $r$  and  $s$ ; and the lines  $P$  and  $Q$ , as well as  $R$  and  $S$ :

$$((p, q, r, s; t, b), (P, Q, R, S; T, B)) \mapsto ((q, p, s, r; t, b), (Q, P, S, R; T, B))$$

**Definition.** A **marked box** is an equivalence class of overmarked boxes under this involution.

From now on, let  $\Theta$  be the marked box labelled as in Figure 10.

**Definition.** We introduce the following notations:

- The **top** of  $\Theta$  is the pair  $(t, T)$ .
- The **bottom** of  $\Theta$  is the pair  $(b, B)$ .

- The **distinguished edges** of  $\Theta$  are  $T$  and  $B$ .
- The **distinguished points** of  $\Theta$  are  $t$  and  $b$ .

Now, we introduce the first geometric property of a marked box.

**Definition.** The marked box  $\Theta$  is **convex** if the following conditions hold:

- C1** The points  $p$  and  $q$  separate  $t$  and  $T \cap B$  on the line  $T$ .
- C2** The points  $r$  and  $s$  separate  $b$  and  $T \cap B$  on the line  $B$ .
- C3** The lines  $P$  and  $Q$  separate  $T$  and  $\overline{bt}$  in the pencil of lines through the point  $t$ , in the cyclic ordering of lines through  $t$ .
- C4** The lines  $R$  and  $S$  separate  $B$  and  $\overline{bt}$  in the pencil of lines through the point  $b$ , in the cyclic ordering of lines through  $b$ .

**Lemma 3.1.** *The condition **C1** holds if and only if condition **C4** holds; the condition **C2** holds if and only if condition **C3** holds.*

*Proof.* We prove the first assertion. As illustrated in Figure 11, the four lines  $R$ ,  $S$ ,  $B$ , and  $\overline{bt}$  in the pencil of lines with axis  $b$  intersect the line  $T$  in the points  $q$ ,  $p$ ,  $T \cap B$ , and  $t$ , respectively. Since  $T$  does not pass through  $b$  (by definition of an overmarked box) the first assertion follows from Observation 2.8. The same argument may be used to prove the second assertion.  $\square$

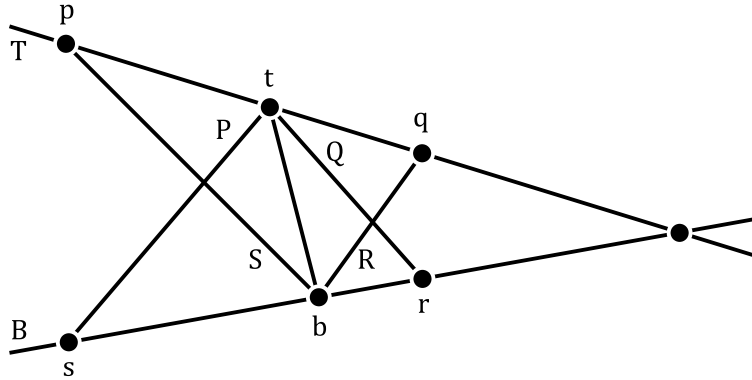


**Figure 11:** Convex marked box that illustrates the proof of Lemma 3.1.

**Definition.** The **convex interior** of the convex marked box  $\Theta$  is the open convex quadrilateral whose vertices, in cyclic order, are  $p$ ,  $q$ ,  $r$ , and  $s$ ; see Figure 12.

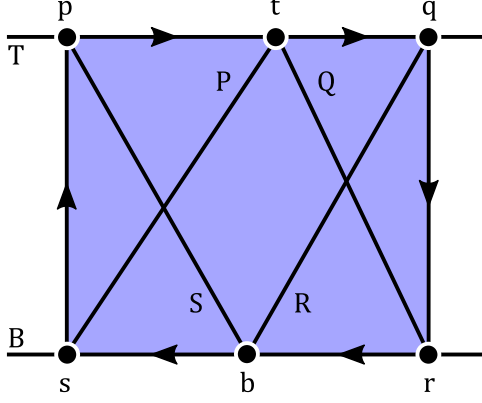


Figure 12: Convex interior of a convex marked box.

### 3.2 Box Operations

To facilitate the definition of box operations, we introduce some notations. If  $p$  and  $q$  are points, then  $pq$  denotes the line through  $p$  and  $q$ . If  $P$  and  $Q$  are lines, then  $PQ$  denotes the point of intersection of  $P$  and  $Q$ .

**Definition.** There are three natural **box operations** on the set of marked boxes. Given

$$\Theta = ((p, q, r, s; t, b), (P, Q, R, S; T, B))$$

as above, we define

$$i(\Theta) = ((s, r, p, q; b, t), (R, S, Q, P; B, T))$$

$$\tau_1(\Theta) = ((p, q, QR, PS; t, (qs)(pr)), (P, Q, qs, pr; T, (QR)(PS)))$$

$$\tau_2(\Theta) = ((QR, PS, s, r; (qs)(pr), b), (pr, qs, S, R; (QR)(PS), B)).$$

Furthermore, we define the identity operation  $1(\Theta) = \Theta$ .

The box operations  $\tau_1$  and  $\tau_2$  explicitly use Pappus' Theorem to generate new marked boxes from the given initial data encoded by the marked box  $\Theta$ . The action of both operations is illustrated in Figure 13.

The box operations may be applied iteratively to form a semigroup  $G$ .

**Lemma 3.2** (Lemma 2.3 in [7]). *The following relations hold for the generators of the semigroup  $G$ :*

$$i^2 = 1, \quad \tau_1 i \tau_2 = i, \quad \tau_2 i \tau_1 = i, \quad \tau_1 i \tau_1 = \tau_2, \quad \text{and} \quad \tau_2 i \tau_2 = \tau_1.$$

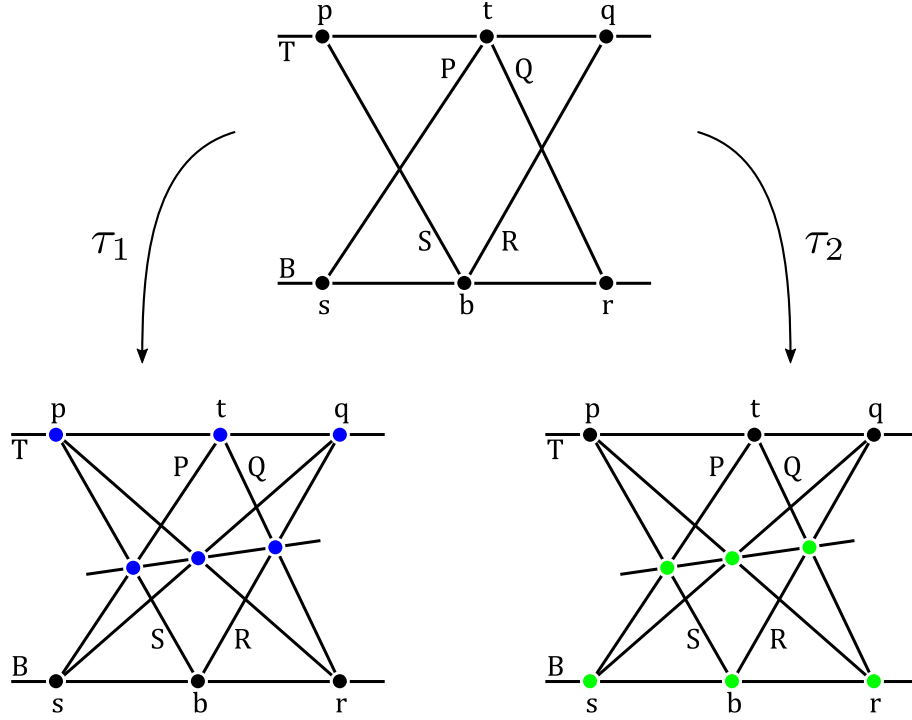


**Figure 13:** Color-coded representation of the box operations  $\tau_1$  and  $\tau_2$ .

**Corollary 3.3.** *The semigroup of box operations  $G$  is a group.*

*Proof.* Using Lemma 3.2, we find the inverse elements of the operations  $i$ ,  $\tau_1$ , and  $\tau_2$  in the semigroup  $G$ , namely,

$$i^{-1} = i, \quad \tau_1^{-1} = i\tau_2i, \quad \text{and} \quad \tau_2^{-1} = i\tau_1i.$$

□

Next, we show that the above-defined box operations preserve convexity.

**Lemma 3.4.** *If  $\Theta$  is a convex marked box, then so are  $i(\Theta)$ ,  $\tau_1(\Theta)$ , and  $\tau_2(\Theta)$ .*

For the proof of Lemma 3.4, we use a projective coordinate system for  $\mathbb{RP}^2$  such that the general position points  $p$ ,  $q$ ,  $r$ , and  $s$  of the marked box  $\Theta$  have the following coordinates:

$$p = (0 : 0 : 1), \quad q = (-1 : 1 : 1), \quad r = (0 : 1 : 0), \quad \text{and} \quad s = (1 : 0 : 0).$$

The coordinates of the top and bottom line are given by

$$T = (1 : 1 : 0) \quad \text{and} \quad B = (0 : 0 : 1)$$

and their point of intersection is

$$TB = (1 : -1 : 0).$$

We parametrize the coordinates of the top and bottom point of  $\Theta$  by

$$\mathbb{R} \cup \{\infty\} \rightarrow T \subset \mathbb{RP}^2, \quad \lambda \mapsto t = (-1 : 1 : 1 + \lambda)$$

and

$$\mathbb{R} \cup \{\infty\} \rightarrow B \subset \mathbb{RP}^2, \quad \mu \mapsto b = (1 : \mu : 0).$$

The coordinates of the remaining lines  $P$ ,  $Q$ ,  $R$ , and  $S$  are given by

$$P = (0 : 1 + \lambda : -1), \quad Q = (1 + \lambda : 0 : 1), \quad R = (\mu : -1 : 1 + \mu), \quad \text{and} \quad S = (\mu : -1 : 0).$$

The following lemma simplifies the proof of Lemma 3.4.

**Lemma 3.5.** *In the above-defined coordinate system, the marked box  $\Theta$  is convex if and only if the parameters  $\lambda$  and  $\mu$  are strictly positive.*

*Proof.* By Lemma 3.1, the marked box  $\Theta$  is convex if and only if it meets conditions **C1** and **C2**. According to Observation 2.5, both conditions are met if and only if the cross-ratios  $[p, q; TB, t]$  and  $[r, s; TB, b]$  are strictly negative. Using the formula for the computation of cross-ratios that is given in Lemma 2.6, we compute:

$$[p, q; TB, t] = \frac{\begin{vmatrix} 1 & 1 \\ 1 + \lambda & 1 \end{vmatrix}}{\begin{vmatrix} 1 & 0 \\ 1 + \lambda & 1 \end{vmatrix}} : \frac{\begin{vmatrix} 1 & 1 \\ 0 & 1 \end{vmatrix}}{\begin{vmatrix} 1 & 0 \\ 0 & 1 \end{vmatrix}} = -\lambda$$

and

$$[r, s; TB, b] = \frac{\begin{vmatrix} 1 & 1 \\ \mu & 0 \end{vmatrix}}{\begin{vmatrix} 1 & 0 \\ \mu & 1 \end{vmatrix}} : \frac{\begin{vmatrix} 1 & 1 \\ -1 & 0 \end{vmatrix}}{\begin{vmatrix} 1 & 0 \\ -1 & 1 \end{vmatrix}} = -\mu.$$

We conclude that both cross-ratios are strictly negative if and only if the parameters  $\lambda$  and  $\mu$  are strictly positive.  $\square$

Now, we prove Lemma 3.4.



*Proof of Lemma 3.4.* First, we show that the marked box

$$i(\Theta) = ((s, r, p, q; b, t), (R, S, Q, P; B, T))$$

meets conditions **C1** and **C2**. For  $i(\Theta)$ , these read as follows:

**C1** The points  $r$  and  $s$  separate  $b$  and  $TB$  on the line  $B$ .

**C2** The points  $p$  and  $q$  separate  $t$  and  $TB$  on the line  $T$ .

We observe that **C1** for  $i(\Theta)$  is the same as **C2** for  $\Theta$ ; and **C2** for  $i(\Theta)$  is the same as **C1** for  $\Theta$ . Hence, the marked box  $i(\Theta)$  is convex, since  $\Theta$  is convex.

Second, we prove that the marked box

$$\tau_1(\Theta) = ((p, q, QR, PS; t, (qs)(pr)), (P, Q, qs, pr; T, (QR)(PS)))$$

is convex. Let  $M = (QR)(PS)$ . Then, the conditions **C1** and **C2** for  $\tau_1(\Theta)$  read as follows:

**C1** The points  $p$  and  $q$  separate  $t$  and  $TM$  on the line  $T$ .

**C2** The points  $QR$  and  $PS$  separate  $(qs)(pr)$  and  $TM$  on the line  $M$ .

We use Observation 2.5 and Lemma 3.5 to show that  $\tau_1(\Theta)$  meets both conditions. The coordinates of the line  $M$  and its point of intersection with the line  $T$  are given by

$$M = (\lambda\mu : 1 : -1) \quad \text{and} \quad TM = (1 : -1 : \lambda\mu - 1).$$

We compute the cross-ratio of the points  $p, q, t$ , and  $TM$ :

$$[p, q; t, TM] = \frac{\begin{vmatrix} -1 & 1 \\ \lambda\mu - 1 & 1 \end{vmatrix}}{\begin{vmatrix} -1 & 0 \\ \lambda\mu - 1 & 1 \end{vmatrix}} : \frac{\begin{vmatrix} 1 & 1 \\ 1 + \lambda & 1 \end{vmatrix}}{\begin{vmatrix} 1 & 0 \\ 1 + \lambda & 1 \end{vmatrix}} = -\mu,$$

which is negative and hence proves condition **C1** for  $\tau_1(\Theta)$ . Similarly, to show that  $\tau_1(\Theta)$  satisfies **C2**, we compute the cross-ratio of the points  $QR, PS, (qs)(pr)$ , and  $TM$ . Their coordinates are given by

$$\begin{aligned} QR &= (1 : \mu - (1 + \lambda)(1 + \mu) : -(1 + \lambda)) \\ PS &= (1 : \mu : \mu(1 + \lambda)) \\ (pr)(qs) &= (0 : 1 : 1). \end{aligned}$$

Their cross-ratio is

$$[PS, QR; (pr)(qs), TM] = \frac{\begin{vmatrix} 1 & 1 \\ \lambda\mu - 1 & -(1 + \lambda) \end{vmatrix}}{\begin{vmatrix} 1 & 1 \\ \lambda\mu - 1 & \mu(1 + \lambda) \end{vmatrix}} : \frac{\begin{vmatrix} 0 & 1 \\ 1 & -(1 + \lambda) \end{vmatrix}}{\begin{vmatrix} 0 & 1 \\ 1 & \mu(1 + \lambda) \end{vmatrix}} = -\lambda,$$

which is also negative. Hence, condition **C2** is satisfied.

Third, we show that the marked box

$$\tau_2(\Theta) = ((QR, PS, s, r; (qs)(pr), b), (pr, qs, S, R; (QR)(PS), B))$$

meets conditions **C1** and **C2**. For  $\tau_2(\Theta)$ , these read as follows:

**C1** The points  $QR$  and  $PS$  separate  $(qs)(pr)$  and  $BM$  on the line  $M$ .

**C2** The points  $s$  and  $r$  separate  $b$  and  $BM$  on the line  $B$ .

We prove the assertion for  $\tau_2(\Theta)$  in the same way as we did for  $\tau_1(\Theta)$ , i.e., by computing cross-ratios. The coordinates of the point of intersection of the lines  $B$  and  $M$  is given by

$$BM = (-1 : \lambda\mu : 0).$$

The cross-ratio of the points  $QR$ ,  $PS$ ,  $(qs)(pr)$ , and  $BM$  is

$$[PS, QR; (pr)(qs), BM] = \frac{\begin{vmatrix} -1 & 1 \\ 0 & -(1 + \lambda) \end{vmatrix}}{\begin{vmatrix} -1 & 1 \\ 0 & \mu(1 + \lambda) \end{vmatrix}} : \frac{\begin{vmatrix} 0 & 1 \\ 1 & -(1 + \lambda) \end{vmatrix}}{\begin{vmatrix} 0 & 1 \\ 1 & \mu(1 + \lambda) \end{vmatrix}} = -\mu^{-1},$$

which is negative. It remains to show that the cross-ratio of the points  $s$ ,  $r$ ,  $b$ , and  $BM$  is negative. We compute:

$$[s, r; b, BM] = \frac{\begin{vmatrix} -1 & 0 \\ \lambda\mu & 1 \end{vmatrix}}{\begin{vmatrix} -1 & 1 \\ \lambda\mu & 0 \end{vmatrix}} : \frac{\begin{vmatrix} 1 & 0 \\ \mu & 1 \end{vmatrix}}{\begin{vmatrix} 1 & 1 \\ \mu & 0 \end{vmatrix}} = -\lambda^{-1},$$

which is also negative and hence completes the proof.  $\square$

The following corollary is an immediate consequence of Lemma 3.4.

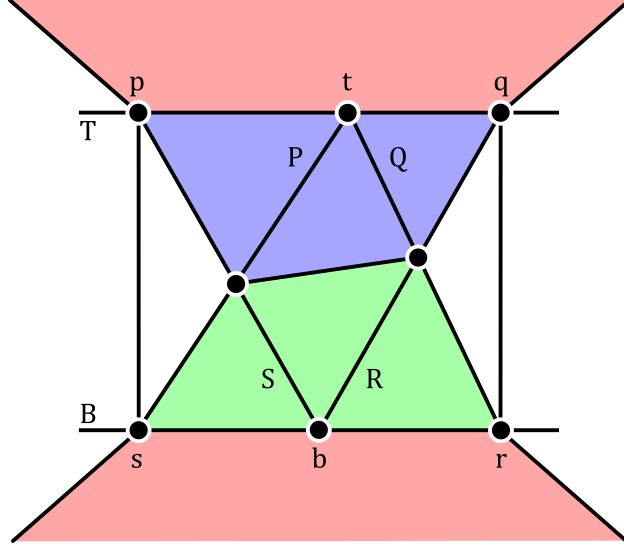


**Figure 14:** Color-coded representation of the convex interiors of the convex marked boxes  $i(\Psi)$  (red),  $\tau_1(\Psi)$  (blue), and  $\tau_2(\Psi)$  (green).

**Corollary 3.6.** *If the marked box  $\Theta$  is convex, then so is every marked box in the orbit  $G(\Theta)$ .*

In the following observation we investigate the so-called nesting property of convex marked boxes in the orbit  $G(\Theta)$ .

**Observation 3.7.** *Let  $\Theta$  be a convex marked box. Given a marked box  $\Psi$  in the orbit  $G(\Theta)$ , the convex interiors of  $\tau_1(\Psi)$  and  $\tau_2(\Psi)$  (the blue and green shaded areas in Figure 14) are nested inside the convex interior of  $\Psi$ . The red shaded area in Figure 14 is the convex interior of  $i(\Psi)$ . The convex interiors of the marked boxes  $i(\Psi)$ ,  $\tau_1(\Psi)$ , and  $\tau_2(\Psi)$  are pairwise disjoint.*

We have collected all the ingredients for the proof of this section's main theorem.

**Theorem 3.8.** *The group of box operations  $G$  is isomorphic to the modular group.*

*Proof.* We use the universal property for generators and relations to show that  $G$  has the presentation  $\langle \alpha, \beta \mid \alpha^2, \beta^3 \rangle$ , which is the presentation of the modular group (as mentioned in Section 2.2).

Let  $S = \{\alpha, \beta\}$  and  $R = \{\alpha^2, \beta^3\} \subset \mathbb{F}(S)$ , where  $\mathbb{F}(S)$  is the free group over the set  $S$ . Let the map  $\phi: S \rightarrow G$  be given by  $\phi(\alpha) = i$  and  $\phi(\beta) = i\tau_1$ . By Lemma 3.2 (relations for the generators of  $G$ ), the set  $R$  is contained in the kernel of the canonical homomorphism  $\bar{\phi}: \mathbb{F}(S) \rightarrow G$ , since  $\bar{\phi}(\alpha^2) = \bar{\phi}(\alpha)^2 = i^2 = 1$  and  $\bar{\phi}(\beta^3) = \bar{\phi}(\beta)^3 = (i\tau_1)^3 = i\tau_1 i\tau_2 = 1$ . By the universal property, there is a unique

homomorphism

$$\phi': \langle S \mid R \rangle \rightarrow G$$

such that  $\phi' \circ \pi = \phi$ , where  $\pi: S \rightarrow \langle S \mid R \rangle$  is the canonical map that takes each element of  $S$  to its equivalence class in  $\langle S \mid R \rangle$ .

Since the group  $G$  is generated by  $\bar{\phi}(\alpha) = i$  and  $\bar{\phi}(\beta) = i\tau_1$  (see Lemma 3.2), the homomorphism  $\phi'$  is surjective. It remains to show that  $\phi'$  is injective. We prove this statement by contradiction. We assume that the kernel of  $\phi'$  is non-trivial. Non-trivial elements in  $\langle S \mid R \rangle$  are represented by one of the following words:

$$\begin{aligned} w_1 &= \alpha\beta^{n_1}\alpha\beta^{n_2}\alpha \dots \alpha\beta^{n_r}\alpha & w_2 &= \alpha\beta^{n_1}\alpha\beta^{n_2}\alpha \dots \alpha\beta^{n_r} \\ w_3 &= \beta^{n_1}\alpha\beta^{n_2}\alpha \dots \alpha\beta^{n_r}\alpha & w_4 &= \beta^{n_1}\alpha\beta^{n_2}\alpha \dots \alpha\beta^{n_r} \end{aligned}$$

with  $n_s \in \{1, 2\}$  for  $s = 1, 2, \dots, r$ . To compute the images of the words  $w_j$  under  $\phi'$  we use the images of  $\alpha\beta$  and  $\alpha\beta^2$ , which are given by

$$\phi'(\alpha\beta) = ii\tau_1 = \tau_1 \quad \text{and} \quad \phi'(\alpha\beta^2) = ii\tau_1i\tau_1 = \tau_2.$$

We compute:

$$\begin{aligned} \phi'(w_1) &= \phi'(\alpha\beta^{n_1}\alpha\beta^{n_2}\alpha \dots \alpha\beta^{n_r}\alpha) \\ &= \phi'(\alpha\beta^{n_1})\phi'(\alpha\beta^{n_2}) \dots \phi'(\alpha\beta^{n_r})\phi'(\alpha) \\ &= \tau_{n_1}\tau_{n_2} \dots \tau_{n_r}i \\ \phi'(w_2) &= \phi'(\alpha\beta^{n_1}\alpha\beta^{n_2}\alpha \dots \alpha\beta^{n_r}) \\ &= \phi'(\alpha\beta^{n_1})\phi'(\alpha\beta^{n_2}) \dots \phi'(\alpha\beta^{n_r}) \\ &= \tau_{n_1}\tau_{n_2} \dots \tau_{n_r} \\ \phi'(w_3) &= \phi'(\beta^{n_1}\alpha\beta^{n_2}\alpha \dots \alpha\beta^{n_r}\alpha) \\ &= \phi'(\alpha^2\beta^{n_1}\alpha\beta^{n_2}\alpha \dots \alpha\beta^{n_r}\alpha) \\ &= \phi'(\alpha)\phi'(\alpha\beta^{n_1})\phi'(\alpha\beta^{n_2}) \dots \phi'(\alpha\beta^{n_r})\phi'(\alpha) \\ &= i\tau_{n_1}\tau_{n_2} \dots \tau_{n_r}i \\ \phi'(w_4) &= \phi'(\beta^{n_1}\alpha\beta^{n_2}\alpha \dots \alpha\beta^{n_r}) \\ &= \phi'(\alpha^2\beta^{n_1}\alpha\beta^{n_2}\alpha \dots \alpha\beta^{n_r}) \\ &= \phi'(\alpha)\phi'(\alpha\beta^{n_1})\phi'(\alpha\beta^{n_2}) \dots \phi'(\alpha\beta^{n_r}) \\ &= i\tau_{n_1}\tau_{n_2} \dots \tau_{n_r}. \end{aligned}$$

Based on the assumption that  $\phi'$  has a non-trivial kernel we conclude that one of the words  $w_j$  is taken to the identity operation in  $G$ , i.e.,  $\phi'(w_j) = 1$ . This implies that either

$$\tau_{n_1}\tau_{n_2}\dots\tau_{n_r} = i \text{ if } j = 1, 4 \quad \text{or} \quad \tau_{n_1}\tau_{n_2}\dots\tau_{n_r} = 1 \text{ if } j = 2, 3.$$

Let  $\Theta$  be a convex marked box. According to Observation 3.7, the convex interior of  $\tau_{n_1}\tau_{n_2}\dots\tau_{n_r}(\Theta)$  and the convex interior of  $i(\Theta)$  are disjoint; and the convex interior of  $\tau_{n_1}\tau_{n_2}\dots\tau_{n_r}(\Theta)$  is a proper subset of the convex interior of  $\Theta$ .

Hence, our assumption, saying that the kernel of  $\phi'$  is non-trivial, is false, which completes the proof of the theorem.  $\square$

The following corollary is an immediate consequence of Theorem 3.8.

**Corollary 3.9.** *Any non-trivial box operation can be represented by one of the following words:*

$$\tau_{n_1}\tau_{n_2}\dots\tau_{n_r}, \quad \tau_{n_1}\tau_{n_2}\dots\tau_{n_r}i, \quad i\tau_{n_1}\tau_{n_2}\dots\tau_{n_r}, \quad \text{or} \quad i\tau_{n_1}\tau_{n_2}\dots\tau_{n_r}i.$$

### 3.3 Marked Boxes and Projective Symmetries

There is an action of the group of projective symmetries  $\mathcal{G}$  on the set of marked boxes that preserves convexity and commutes with the action of box operations.

**Definition.** Given a projective transformation  $T: \mathbb{RP}^2 \rightarrow \mathbb{RP}^2$  and a duality  $\Delta: \mathbb{RP}^2 \rightarrow (\mathbb{RP}^2)^*$ , let  $\hat{x} = T(x)$  and  $x^* = \Delta(x)$ , where  $x$  is either a point or a line. Given the marked box  $\Theta = ((p, q, r, s; t, b), (P, Q, R, S; T, B))$ , we define

$$\begin{aligned} T(\Theta) &= ((\hat{p}, \hat{q}, \hat{r}, \hat{s}; \hat{t}, \hat{b}), (\hat{P}, \hat{Q}, \hat{R}, \hat{S}; \hat{T}, \hat{B})) \\ \Delta(\Theta) &= ((P^*, Q^*, S^*, R^*; T^*, B^*), (q^*, p^*, r^*, s^*; t^*, b^*)). \end{aligned}$$

First, we show that projective symmetries preserve convexity.

**Lemma 3.10.** *If the marked box  $\Theta$  is convex, then so is its image under a projective symmetry.*

*Proof.* We show that the marked boxes  $T(\Theta)$  and  $\Delta(\Theta)$  meet the convexity conditions from Section 3.1. For  $T(\Theta)$  we prove the conditions **C1** and **C2** and for  $\Delta(\Theta)$  we prove the conditions **C3** and **C4**.

First, for the marked box

$$T(\Theta) = ((\hat{p}, \hat{q}, \hat{r}, \hat{s}; \hat{t}, \hat{b}), (\hat{P}, \hat{Q}, \hat{R}, \hat{S}; \hat{T}, \hat{B}))$$

the conditions **C1** and **C2** read as follows:

**C1** The points  $\hat{p}$  and  $\hat{q}$  separate  $\hat{t}$  and  $\widehat{TB}$  on the line  $\hat{T}$ .

**C2** The points  $\hat{r}$  and  $\hat{s}$  separate  $\hat{b}$  and  $\widehat{TB}$  on the line  $\hat{B}$ .

Since the marked box  $\Theta$  is convex it satisfies the conditions **C1** and **C2**. Consequently, by Observation 2.5, the cross-ratios  $[p, q; t, TB]$  and  $[r, s; b, TB]$  are negative. As projective transformations preserve cross-ratios (see Lemma 2.4), we conclude that the ratios  $[\hat{p}, \hat{q}; \hat{t}, \widehat{TB}]$  and  $[\hat{r}, \hat{s}; \hat{b}, \widehat{TB}]$  are negative. Hence, the marked box  $T(\Theta)$  meets **C1** and **C2**.

Second, for the marked box

$$\Delta(\Theta) = ((P^*, Q^*, S^*, R^*; T^*, B^*), (q^*, p^*, r^*, s^*; t^*, b^*))$$

the conditions **C3** and **C4** are as follows:

**C3** The lines  $q^*$  and  $p^*$  separate  $t^*$  and  $T^*B^*$  in the pencil of lines through the point  $T^*$ , in the cyclic ordering of lines through  $T^*$ .

**C4** The lines  $r^*$  and  $s^*$  separate  $b^*$  and  $T^*B^*$  in the pencil of lines through the point  $B^*$ , in the cyclic ordering of lines through  $B^*$ .

By Observation 2.9, the marked box  $\Delta(\Theta)$  is convex if the cross-ratios  $[q^*, p^*; t^*, T^*B^*]$  and  $[r^*, s^*; b^*, T^*B^*]$  are negative. Since dualities are projective transformations from  $\mathbb{RP}^2$  to  $(\mathbb{RP}^2)^*$  (and thus preserve cross-ratios), and  $\Theta$  meets conditions **C1** and **C2**, we conclude that  $\Delta(\Theta)$  is a convex marked box.  $\square$

**Lemma 3.11.** *The actions of projective symmetries and box operations commute.*

*Proof.* To show that projective transformations  $T$  commute with box operations in  $G$ , it suffices to prove that  $T$  commutes with the operations  $i$  and  $\tau_1$ , since  $i$  and  $i\tau_1$  generate  $G$  (see Lemma 3.2). We compute:

$$\begin{aligned} T(i(\Theta)) &= ((\hat{s}, \hat{r}, \hat{p}, \hat{q}; \hat{b}, \hat{t}), (\hat{R}, \hat{S}, \hat{Q}, \hat{P}; \hat{B}, \hat{T})) \\ &= i(T(\Theta)) \end{aligned}$$

$$\begin{aligned} T(\tau_1(\Theta)) &= ((\hat{p}, \hat{q}, \widehat{QR}, \widehat{PS}; \hat{t}, (\widehat{qs})(\widehat{pr})), (\hat{P}, \hat{Q}, \widehat{qs}, \widehat{pr}; \hat{T}, (\widehat{QR})(\widehat{PS}))) \\ &= ((\hat{p}, \hat{q}, \hat{Q}\hat{R}, \hat{P}\hat{S}; \hat{t}, (\hat{q}\hat{s})(\hat{p}\hat{r})), (\hat{P}, \hat{Q}, \hat{q}\hat{s}, \hat{p}\hat{r}; \hat{T}, (\hat{Q}\hat{R})(\hat{P}\hat{S}))) \\ &= \tau_1(T(\Theta)). \end{aligned}$$

In the same way, we show that dualities  $\Delta$  commute with box operations:

$$\begin{aligned}
\Delta(i(\Theta)) &= ((R^*, S^*, P^*, Q^*, B^*, T^*), (r^*, s^*, p^*, q^*, b^*, t^*)) \\
&= i(\Delta(\Theta)) \\
\Delta(\tau_1(\Theta)) &= ((P^*, Q^*, pr^*, qs^*, T^*, (QR)(PS)^*), \\
&\quad (q^*, p^*, QR^*, PS^*, t^*, (qs)(pr)^*)) \\
&= ((P^*, Q^*, p^*r^*, q^*s^*, T^*, (Q^*R^*)(P^*S^*)), \\
&\quad (q^*, p^*, Q^*R^*, P^*S^*, t^*, (p^*r^*)(q^*s^*))) \\
&= \tau_1(\Delta(\Theta)).
\end{aligned}$$

This completes the proof.  $\square$

Thus far, we have defined two commuting group actions on the set of marked boxes that preserve convexity, the action of box operations as well as the action of projective symmetries.

For the remainder of this section, let  $\Theta$  be a convex marked box and let  $\Omega = G(\Theta)$  be its orbit under the action of the group of box operations  $G$ . In the following, we investigate symmetries of  $\Omega$ , i.e., transformations that preserve the orbit. The first step is to identify the elements in  $G$  with the elements in  $\Omega$ . Naturally, the action of  $G$  on  $\Omega$  is transitive. In the next lemma, we show that the action is free.

**Lemma 3.12.** *The group of box operations  $G$  acts freely on  $\Omega$ .*

*Proof.* We assume that  $G$  does not act freely on  $\Omega$ . Then, there is a marked box  $\Psi \in \Omega$  and a box operation  $g \in G$ , which is not the identity operation, such that  $g$  fixes  $\Psi$ . However, in the proof of Theorem 3.8 we showed that no non-trivial box operation fixes a convex marked box (all marked boxes in  $\Omega$  are convex since box operations preserve convexity), which is a contradiction to our assumption.  $\square$

**Corollary 3.13.** *There is a natural bijection between  $G$  and  $\Omega$ .*

*Proof.* The action of  $G$  on  $\Omega$  is transitive and free.  $\square$

Next, we represent  $\Omega$  by a directed graph  $\Gamma$ . Schwartz describes the identification as follows: “The edges of  $\Gamma$  correspond to marked boxes in  $\Omega$ , the vertices correspond to tops and bottoms of marked boxes, and each edge is directed from the top to the bottom. Vertices on distinct edges are identified if the corresponding distinguished sides of the marked boxes coincide.”

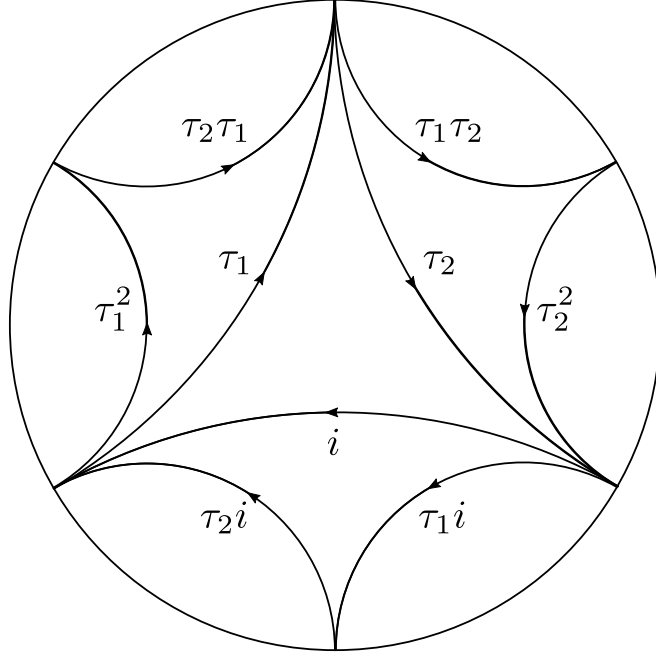


**Figure 15:** Embedding of the graph  $\Gamma$  into the hyperbolic plane.

We embed  $\Gamma$  in the real hyperbolic plane as the tiling associated with the group which is generated by the reflections in the sides of an ideal triangle (cf. Section 2.2). Figure 15 illustrates a finite portion of the graph where the edges are labelled by elements of  $G$ .

Furthermore, Schwartz points out that “the group of box operations acts as a group of permutations on the edges of  $\Gamma$ . The operation  $i$  reverses the orientation on each edge. The element  $\tau_1$  rotates each edge counterclockwise one click about its tail point. The element  $\tau_2$  rotates each edge one click clockwise about its head point.”

As described in Section 2.2, the modular group is generated by an order three rotation  $R_3$  about the center of the triangle bounded by the edges  $i$ ,  $\tau_1$ , and  $\tau_2$ , and an order two rotation  $R_2$  about the center of the edge  $i$ . Hence, there is an action of the modular group on  $\Gamma$  as a group of graph-isomorphisms induced by hyperbolic isometries. Since the edges of  $\Gamma$  are in bijection with the marked boxes in the orbit  $\Omega$ , these graph-isomorphisms translate into symmetries of  $\Omega$ .

The order three rotation  $R_3$  has the cycle

$$i(\Theta) \xrightarrow{R_3} \tau_1(\Theta) \xrightarrow{R_3} \tau_2(\Theta) \xrightarrow{R_3} i(\Theta)$$

and the order two rotation  $R_2$  has the cycle

$$\Theta \xrightarrow{R_2} i(\Theta) \xrightarrow{R_2} \Theta.$$



In the following, we show that there are also projective symmetries of the orbit  $\Omega$ . We begin by showing that there are projective symmetries that have the same cycles as the hyperbolic rotations  $R_2$  and  $R_3$ .

**Lemma 3.14.** *For any marked box  $\Theta$  there is an order three projective transformation  $T$  having the cycle*

$$i(\Theta) \xrightarrow{T} \tau_1(\Theta) \xrightarrow{T} \tau_2(\Theta) \xrightarrow{T} i(\Theta)$$

and a polarity  $\Delta$  having the cycle

$$\Theta \xrightarrow{\Delta} i(\Theta) \xrightarrow{\Delta} \Theta.$$

*Proof.* Let the marked box  $\Theta$  be given by

$$\Theta = ((p, q, r, s; t, b), (P, Q, R, S; T, B)).$$

First, we define the projective transformation  $T$  by

$$T(s) = p, \quad T(r) = q, \quad T(p) = QR, \quad \text{and} \quad T(q) = PS.$$

Using the coordinate system that we introduced for the proof of Lemma 3.4, the projective transformation  $T$  can be represented by the matrix

$$T = \begin{pmatrix} 0 & \lambda + 1 & & -1 \\ 0 & -(\lambda + 1) & (\lambda + 1)(\mu + 1) - \mu & \\ -(\lambda + 1)\lambda\mu & -(\lambda + 1) & & \lambda + 1 \end{pmatrix}.$$

A straightforward matrix-vector multiplication shows that  $T$  has the cycles

$$\begin{array}{ccccccc} s & \xrightarrow{T} & p & \xrightarrow{T} & QR & \xrightarrow{T} & s \\ r & \xrightarrow{T} & q & \xrightarrow{T} & PS & \xrightarrow{T} & r \\ b & \xrightarrow{T} & t & \xrightarrow{T} & (qs)(pr) & \xrightarrow{T} & b. \end{array}$$

We conclude that the transformation  $T$  has the cycle

$$i(\Theta) \xrightarrow{T} \tau_1(\Theta) \xrightarrow{T} \tau_2(\Theta) \xrightarrow{T} i(\Theta),$$

which can be seen by writing the marked boxes  $i(\Theta)$ ,  $\tau_1(\Theta)$ ,  $\tau_2(\Theta)$ , and  $i(\Theta)$  one below the other (recall that a projective transformation does not permute the

points and lines of a marked box):

$$\begin{aligned}
i(\Theta) &= ((s, r, p, q; b, t), (\dots)) \\
\tau_1(\Theta) &= ((p, q, QR, PS; t, (qs)(pr)), (\dots)) \\
\tau_2(\Theta) &= ((QR, PS, s, r; (qs)(pr), b), (\dots)) \\
i(\Theta) &= ((s, r, p, q; b, t), (\dots)).
\end{aligned}$$

It is sufficient to prove the assertion for the points of the marked boxes, since the lines of a marked box are determined by its points and  $T$  is a projective transformation of  $\mathbb{RP}^2$ , which preserves incidence relations.

From the cycles of points we also conclude that  $T$  is a transformation of order three, since  $T^3$  fixes the projective basis  $(p, q, r, s)$  of  $\mathbb{RP}^2$ .

Second, we define the duality  $\Delta$  by

$$\Delta(p) = R, \quad \Delta(q) = S, \quad \Delta(r) = P, \quad \text{and} \quad \Delta(s) = Q.$$

Using the same coordinate system as above,  $\Delta$  can be represented by the following matrix:

$$\Delta = \begin{pmatrix} -(\lambda + 1)\mu & 0 & -\mu \\ 0 & -(\lambda + 1) & 1 \\ -\mu & 1 & -(\mu + 1) \end{pmatrix}.$$

Again, a straightforward matrix-vector multiplication shows that

$$\Delta(t) = B \quad \text{and} \quad \Delta(b) = T.$$

This proves that the duality  $\Delta$  has the cycle

$$\Theta \xrightarrow{\Delta} i(\Theta) \xrightarrow{\Delta} \Theta,$$

which can be seen from the stack of marked boxes below:

$$\begin{aligned}
\Delta(\Theta) &= ((\dots), (p^*, q^*, s^*, r^*; t^*, b^*)) \\
i(\Theta) &= ((\dots), (R, S, Q, P; B, T)) \\
\Delta(i(\Theta)) &= ((\dots), (r^*, s^*, p^*, q^*, b^*, t^*)) \\
\Theta &= ((\dots), (P, Q, R, S; T, B)).
\end{aligned}$$

Analogous to the first part of the proof, where we showed the assertion only for the points of a marked box, here, we use the lines of the boxes above. This is

also sufficient, since the points of a marked box can be defined as the points of intersection of its lines, and dualities also preserve incidence relations.

The duality  $\Delta$  is a polarity since  $\Delta^2$  leaves the projective basis  $(p, q, r, s)$  of  $\mathbb{RP}^2$  invariant:

$$\begin{aligned}\Delta^2(p) &= \Delta(R) = \Delta(bq) = \Delta(b)\Delta(q) = TS = p \\ \Delta^2(q) &= \Delta(S) = \Delta(bp) = \Delta(b)\Delta(p) = TR = q \\ \Delta^2(r) &= \Delta(P) = \Delta(ts) = \Delta(t)\Delta(s) = BQ = r \\ \Delta^2(s) &= \Delta(Q) = \Delta(tr) = \Delta(t)\Delta(r) = BP = s.\end{aligned}$$

This completes the proof. □

The next corollary facilitates the proof of this section's main theorem.

**Corollary 3.15.** *The following equations hold:*

$$\Delta(\Theta) = i(\Theta), \quad T(\Theta) = i\tau_1(\Theta), \quad T\Delta(\Theta) = \tau_1(\Theta), \quad \text{and} \quad T^2\Delta(\Theta) = \tau_2(\Theta).$$

*Proof.* Using the definition of the projective transformation  $T$  and the duality  $\Delta$  for the marked box  $\Theta$ , and the fact that projective symmetries commute with box operations (see Lemma 3.11), we compute:

$$\Delta(\Theta) = i(\Theta) \quad \text{and} \quad T(\Theta) = T(ii\Theta) = iT(i(\Theta)) = i\tau_1(\Theta).$$

Thereon, we also get

$$T\Delta(\Theta) = T(i(\Theta)) = \tau_1(\Theta) \quad \text{and} \quad T^2\Delta(\Theta) = T^2(i(\Theta)) = \tau_2(\Theta). \quad \square$$

Lemma 3.14 implies that any marked box  $\Theta$  induces a representation of the modular group  $M$ , which has the presentation  $\langle \alpha, \beta \mid \alpha^2, \beta^3 \rangle$ , into the group of projective symmetries:

$$\bar{M}: M \rightarrow \mathcal{G}, \quad \text{given by } \bar{M}(\alpha) = \Delta \text{ and } \bar{M}(\beta) = T.$$

**Lemma 3.16.** *The image of  $\bar{M}$  is a group of projective symmetries of  $\Omega$ .*

*Proof.* Let  $g \in G$  be a box operation and let  $\Psi = g(\Theta)$ . Then, using Corollary 3.15, we get  $T(\Psi) = gi\tau_1(\Theta)$  and  $\Delta(\Psi) = gi(\Theta)$ , which shows that  $T(\Psi)$  and  $\Delta(\Psi)$  are elements of  $\Omega$ . □

Now, we prove the main theorem of this section.

**Theorem 3.17.** *If the marked box  $\Theta$  is convex, then the representation  $\overline{M}: M \rightarrow \mathcal{G}$  is faithful.*

*Proof.* The structure of this proof is similar to the structure of the proof of Theorem 3.8, where we showed that the group of box operations is isomorphic to the modular group.

To prove the assertion, we assume that the representation  $\overline{M}$  is not faithful, i.e.,  $\overline{M}$  takes a non-identity element in  $M$  to the identity in  $\mathcal{G}$ . The following words represent non-identity elements in  $M$ :

$$\begin{aligned} w_1 &= \alpha\beta^{n_1}\alpha\beta^{n_2}\alpha \dots \alpha\beta^{n_r}\alpha & w_2 &= \alpha\beta^{n_1}\alpha\beta^{n_2}\alpha \dots \alpha\beta^{n_r} \\ w_3 &= \beta^{n_1}\alpha\beta^{n_2}\alpha \dots \alpha\beta^{n_r}\alpha & w_4 &= \beta^{n_1}\alpha\beta^{n_2}\alpha \dots \alpha\beta^{n_r} \end{aligned}$$

where  $n_s \in \{1, 2\}$  for  $s = 1, 2, \dots, r$ . The images of the  $w_j$  under  $\overline{M}$  are given by

$$\begin{aligned} \overline{M}(w_1) &= \Delta T^{n_1} \Delta T^{n_2} \Delta \dots \Delta T^{n_r} \Delta & \overline{M}(w_2) &= \Delta T^{n_1} \Delta T^{n_2} \Delta \dots \Delta T^{n_r} \\ \overline{M}(w_3) &= T^{n_1} \Delta T^{n_2} \Delta \dots \Delta T^{n_r} \Delta & \overline{M}(w_4) &= T^{n_1} \Delta T^{n_2} \Delta \dots \Delta T^{n_r}. \end{aligned}$$

By our assumption, there is a word  $w_j$  such that  $\overline{M}(w_j) = 1$ . Consequently, the projective symmetry  $\overline{M}(w_j)$  fixes the convex marked box  $\Theta$ , and the convex interior of  $\overline{M}(w_j)(\Theta)$  agrees with the convex interior of  $\Theta$ . However, if we compute the image of  $\Theta$  under the projective symmetries  $\overline{M}(w_j)$ , using Corollary 3.15, we get

$$\begin{aligned} \overline{M}(w_1)(\Theta) &= \Delta T^{n_1} \Delta T^{n_2} \Delta \dots \Delta T^{n_r} \Delta(\Theta) \\ &= \tau_{n_r} \tau_{n_{r-1}} \dots \tau_{n_1} i(\Theta) \\ \overline{M}(w_2)(\Theta) &= \Delta T^{n_1} \Delta T^{n_2} \Delta \dots \Delta T^{n_r}(\Theta) \\ &= i \tau_{n_r} \tau_{n_{r-1}} \dots \tau_{n_1} i(\Theta) \\ \overline{M}(w_3)(\Theta) &= T^{n_1} \Delta T^{n_2} \Delta \dots \Delta T^{n_r} \Delta(\Theta) \\ &= \tau_{n_r} \tau_{n_{r-1}} \dots \tau_{n_1}(\Theta) \\ \overline{M}(w_4)(\Theta) &= T^{n_1} \Delta T^{n_2} \Delta \dots \Delta T^{n_r}(\Theta) \\ &= i \tau_{n_r} \tau_{n_{r-1}} \dots \tau_{n_1}(\Theta). \end{aligned}$$

As in the proof of Theorem 3.8, this contradicts the nesting properties of convex marked boxes.  $\square$

## 4 Pappus Curves

Let  $\Theta$  be a convex marked box and let  $\Omega$  be its orbit under the action of the group of box operations  $G$  as defined in Section 3.3. Schwartz [7] proves that the distinguished points, i.e., the top and bottom points, of marked boxes in  $\Omega$  are dense in a topological circle  $\Lambda$ , a so-called Pappus Curve, in  $\mathbb{RP}^2$ .

The set of distinguished points of marked boxes in  $\Omega$  can be computed by recursively applying the box operations  $\tau_1$  and  $\tau_2$  to the marked boxes  $\Theta$  and  $i(\Theta)$ . Let  $B_0 = \{\Theta, i(\Theta)\}$ . For  $j > 0$ , we recursively define the sets  $B_j$  such that  $B_j$  contains the marked box  $\Psi$  if there is a marked box  $\Phi \in B_{j-1}$  such that  $\Psi = \tau_1(\Phi)$  or  $\Psi = \tau_2(\Phi)$ , i.e.,

$$B_j = \{\Psi \mid \exists \Phi \in B_{j-1} : \Psi = \tau_1(\Phi) \vee \Psi = \tau_2(\Phi)\}.$$

Let  $P_j$  be the set that contains the distinguished points of marked boxes in  $B_j$ . Then,  $\bigcup_{j=0}^{\infty} P_j$  is dense in  $\Lambda$ .

In his dissertation “Algebraic Pappus Curves” [5], Tatsuhiko Hatase shows that a Pappus Curve is algebraic if and only if it is linear (where algebraic means that the points of the Pappus Curve satisfy an irreducible polynomial equation). Figure 16 illustrates a linear Pappus Curve in the sphere model for  $\mathbb{RP}^2$  (the blue circle on the right) as well as the corresponding initial marked box  $\Theta$  that is symmetric with respect to the line  $\Lambda$ .

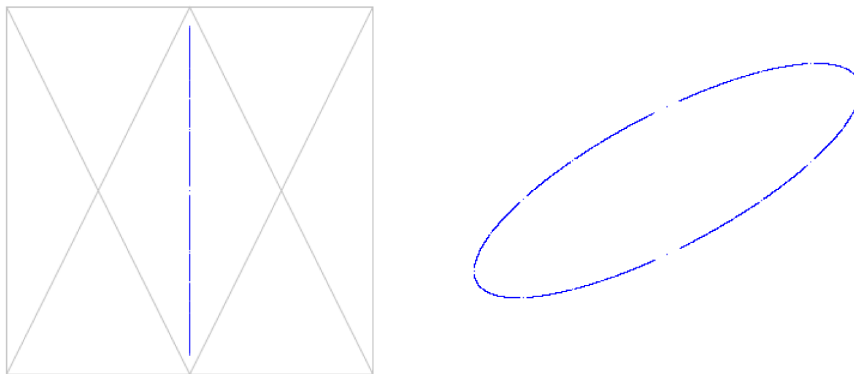


**Figure 16:** Symmetric marked box and linear Pappus Curve.

If we break the symmetry of  $\Theta$ , e.g., by varying the positions of its top and bottom point, the resulting Pappus Curve exhibits edges and sharp bends; see Figure 17. Even if we magnify a small part of the curve (the images on the left side in Figure 17 show the parts of the Pappus Curves that are contained in the convex interior of  $\Theta$ ) we notice a very detailed and edgy structure.

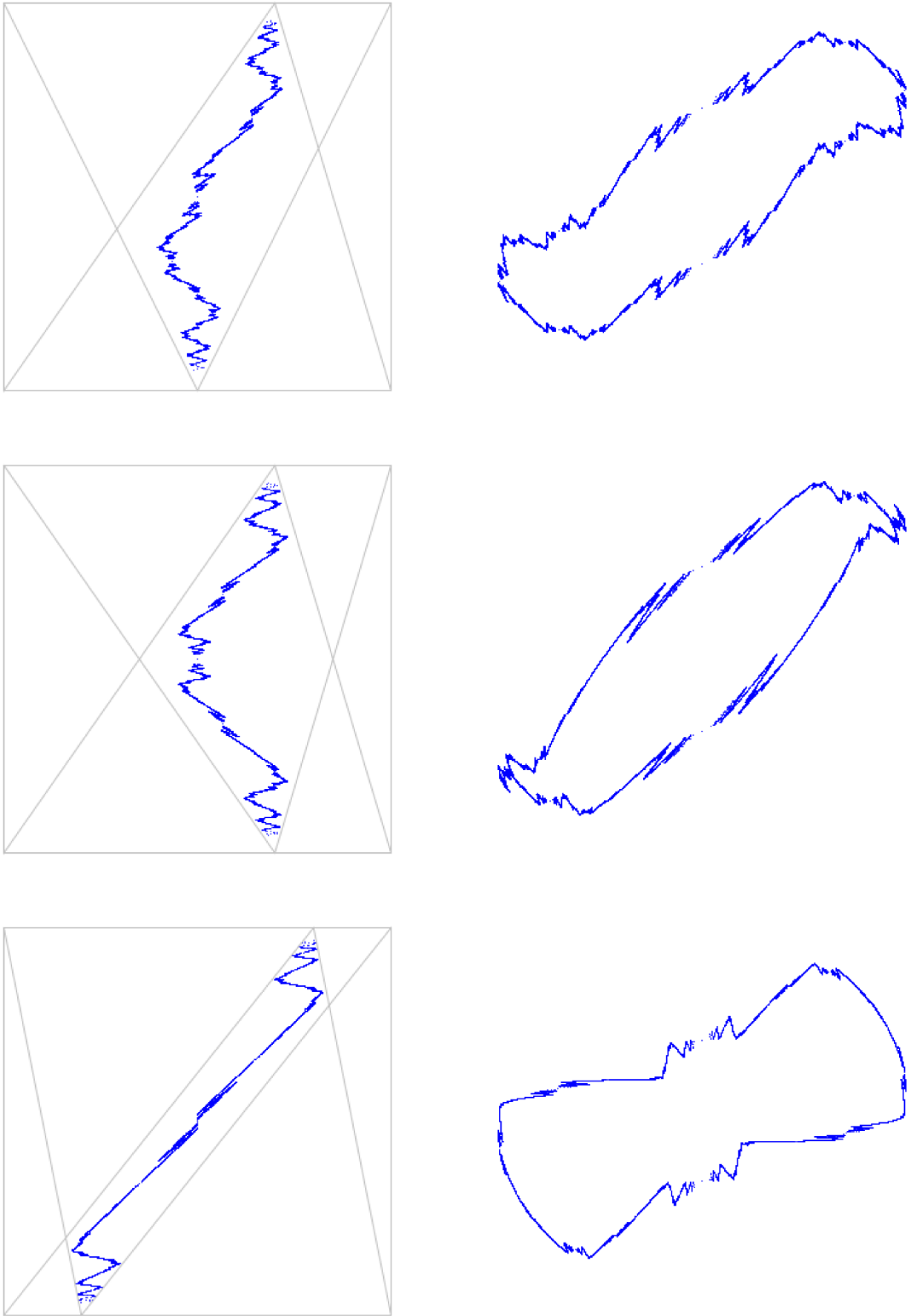


**Figure 17:** Pappus Curves that correspond to non-symmetric marked boxes.

The above-mentioned properties of Pappus Curves (they are defined recursively and they have a fine and detailed structure that is difficult to describe if they are not linear) are, according to Kenneth Falconer [2], typical features of fractal sets.

In the following sections, we show that Pappus Curves have two additional characteristics of fractal sets: They are self-similar and their box dimension is greater than their topological dimension, which is equal to one, since Pappus Curves are homeomorphic to a circle.

## 4.1 Self-Similarity

In Lemma 3.16, we showed that  $\overline{M}$  is a group of projective symmetries of  $\Omega$ . The subgroup of projective transformations  $\overline{M}' \subset \overline{M}$  is a group of automorphisms of  $\Lambda$ .

**Lemma 4.1.** *The group  $\overline{M}'$  is an index 2 subgroup of  $\overline{M}$ .*

*Proof.* Let  $S \in \overline{M}$  be a projective symmetry and let  $w = w(T, \Delta)$  be the word in the generators of  $\overline{M}$  that represents  $S$ . Since projective transformations take points to points and lines to lines, and dualities take points to lines and lines to points,  $S$  acts on the real projective plane as a projective transformation if and only if  $w$  contains an even number of dualities  $\Delta$ . Therefore, there are exactly two cosets of  $\overline{M}'$  in  $\overline{M}$ , namely  $\overline{M}'$  and  $\Delta\overline{M}'$ ; the latter contains the dualities in  $\overline{M}$ .  $\square$

Our next goal is to show that Pappus Curves are projectively self-similar.

**Lemma 4.2.** *Let  $S_1 = T\Delta T\Delta$ ,  $S_2 = T\Delta T^2\Delta$ ,  $S_3 = T^2\Delta T\Delta$ , and  $S_4 = T^2\Delta T^2\Delta$ . These projective transformations take the marked box  $\Theta$  to  $\tau_1\tau_1(\Theta)$ ,  $\tau_2\tau_1(\Theta)$ ,  $\tau_1\tau_2(\Theta)$ , and  $\tau_2\tau_2(\Theta)$ , respectively; see Figure 18.*

*Proof.* The assertion follows from Corollary 3.15.  $\square$

For an arbitrary box operation  $g \in G$ , let  $P_g \in \overline{M}$  be the projective symmetry such that  $g(\Theta) = P_g(\Theta)$ . A suitable symmetry  $P_g$  exists according to Corollary 3.15.

**Lemma 4.3.** *The projective transformations  $P_g S_1 P_g^{-1}$ ,  $P_g S_2 P_g^{-1}$ ,  $P_g S_3 P_g^{-1}$ , and  $P_g S_4 P_g^{-1}$  take the marked box  $g(\Theta)$  to  $\tau_1\tau_1(g(\Theta))$ ,  $\tau_2\tau_1(g(\Theta))$ ,  $\tau_1\tau_2(g(\Theta))$ , and  $\tau_2\tau_2(g(\Theta))$ , respectively.*

*Proof.* First, we clarify that the projective symmetries  $P_g S_j P_g^{-1}$  are projective transformations. We distinguish two cases:

- If  $P_g$  is a projective transformation then so is  $P_g^{-1}$ , and  $P_g S_j P_g^{-1}$  is a conjunction of projective transformations.

- If  $P_g$  is a duality then so is  $P_g^{-1}$ . Let  $w = w(\mathbb{T}, \Delta)$  be the word in the generators of  $\overline{\mathbb{M}}$  that represents  $P_g$ . The number of dualities  $\Delta$  in  $w$  and  $w^{-1}$  is odd. Consequently, the number of dualities  $\Delta$  in the word in the generators of  $\overline{\mathbb{M}}$  that represents  $P_g S_j P_g^{-1}$  is even, which means that the latter acts on  $\mathbb{RP}^2$  as a projective transformation.

Using Lemma 4.2, we compute that the projective transformation  $P_g S_1 P_g^{-1}$  takes  $g(\Theta)$  to  $\tau_1 \tau_1(g(\Theta))$ :

$$\begin{aligned}
P_g S_1 P_g^{-1}(g(\Theta)) &= g(P_g S_1 P_g^{-1}(\Theta)) \\
&= g(P_g S_1(g^{-1}(\Theta))) \\
&= g g^{-1}(P_g S_1(\Theta)) \\
&= P_g(\tau_1 \tau_1(\Theta)) \\
&= \tau_1 \tau_1(P_g(\Theta)) \\
&= \tau_1 \tau_1(g(\Theta))
\end{aligned}$$

The remaining assertions may be proven in the same way. □

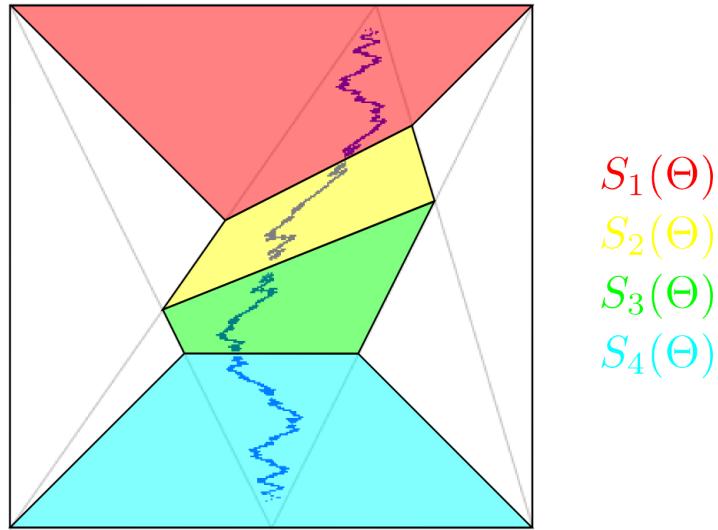


**Figure 18:** Color-coded representation of the marked boxes  $S_j(\Theta)$ .

Let  $\Psi \in \Omega$  be an arbitrary marked box. By  $\Lambda_\Psi$  we denote the intersection of the Pappus Curve associated with  $\Omega$  and the closure of the open convex interior of  $\Psi$ .

Now, we prove this section's main theorem.



**Theorem 4.4.** For all box operations  $g \in G$  the segment  $\Lambda_{g(\Theta)}$  of the Pappus Curve  $\Lambda$  is projectively similar to the four smaller segments  $\Lambda_{P_g S_j P_g^{-1}(g(\Theta))}$  where  $1 \leq j \leq 4$ , i.e.,

$$\Lambda_{g(\Theta)} = \bigcup_{j=1}^4 \Lambda_{P_g S_j P_g^{-1}(g(\Theta))}.$$

*Proof.* The assertion follows from Lemma 4.3 and the fact that the projective transformations  $P_g S_j P_g^{-1}$  are automorphisms of  $\Lambda$ , which implies that

$$P_g S_j P_g^{-1}(\Lambda_{g(\Theta)}) = \Lambda_{P_g S_j P_g^{-1}(g(\Theta))}.$$

□

## 4.2 Box Dimension

This section is based on Chapter 3 of Kenneth Falconer's book "Fractal Geometry" [2].

### 4.2.1 Definition and Algorithmic Approach

According to Falconer, "the idea of measurement at scale  $\delta$  is fundamental to the definition of box dimension. For each  $\delta$ , we measure a set in a way that ignores irregularities of size less than  $\delta$ , and we see how these measurements behave as  $\delta$  tends to zero".

First, we define the box dimension of a bounded subset of  $\mathbb{R}^n$ . From this definition we then derive an algorithm for its numerical approximation.

**Definition.** Let  $F$  be any non-empty bounded subset of  $\mathbb{R}^n$ . Consider the collection of cubes in the  $\delta$ -coordinate mesh of  $\mathbb{R}^n$ , i.e., cubes of the form

$$[m_1\delta, (m_1 + 1)\delta] \times [m_2\delta, (m_2 + 1)\delta] \times \dots \times [m_n\delta, (m_n + 1)\delta]$$

where  $m_1, m_2, \dots, m_n$  are integers. Let  $N_\delta(F)$  be the number of  $\delta$ -mesh cubes that intersect  $F$  as shown in Figure 19. The **lower** and **upper box dimension** of  $F$  are then given by

$$\underline{\dim}_B F = \liminf_{\delta \rightarrow 0} \frac{\log N_\delta(F)}{-\log \delta},$$

$$\overline{\dim}_B F = \limsup_{\delta \rightarrow 0} \frac{\log N_\delta(F)}{-\log \delta}.$$

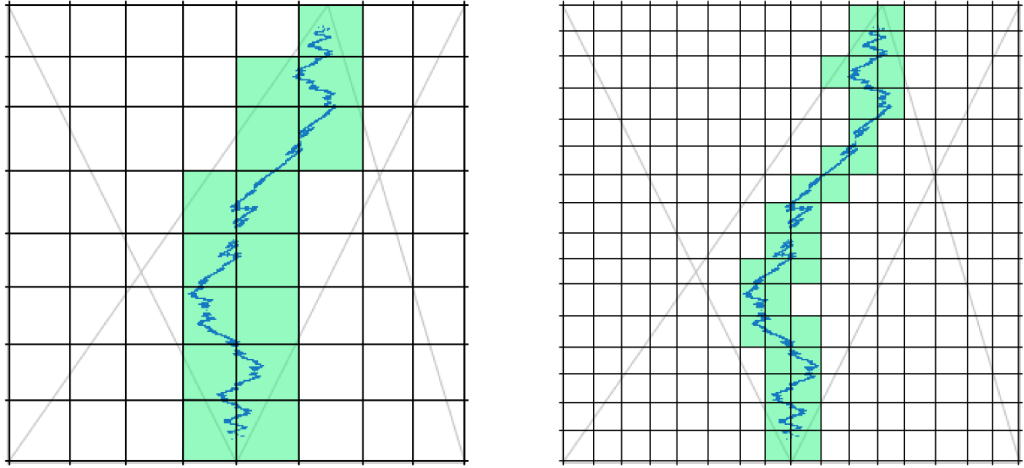


**Figure 19:** Squares in  $\delta$ -coordinate meshes that intersect  $\Lambda_\Theta$ .

If these are equal we refer to the common value as the **box dimension** of  $F$

$$\dim_B F = \lim_{\delta \rightarrow 0} \frac{\log N_\delta(F)}{-\log \delta}.$$

The following examples are from Sections 3.1 and 3.2 in [2].

**Example 4.1.** Let  $F$  be as in the definition above. The box dimension of  $F$  is an upper bound for the Hausdorff dimension of  $F$ , i.e.,

$$\dim_H F \leq \underline{\dim}_B F \leq \overline{\dim}_B F.$$

Equality holds, for example, if  $F$  is a bounded smooth  $m$ -dimensional submanifold of  $\mathbb{R}^n$ . In this case, we have  $\dim_H F = \dim_B F = m$ . If  $F$  is the set of rational numbers in the compact interval  $[0, 1] \subset \mathbb{R}$ , then  $\dim_H F = 0$  and  $\dim_B F = 1$ .

We may interpret the last equation in the definition of box dimension as follows. If  $\delta$  is close to zero, then there is an almost linear relationship

$$\log N_\delta(F) \approx -s \log \delta,$$

where  $s$  is the box dimension of  $F$ . From this observation we derive an algorithm for the numerical approximation of  $\dim_B F$ , where the underlying idea is to estimate the gradient of the graph of  $\log N_\delta(F)$  against  $-\log \delta$ .

Falconer says that “the number of mesh cubes of size  $\delta$  that intersect a set is an indication of how spread out or irregular the set is when examined at scale  $\delta$ . The dimension reflects how rapidly the irregularities develop as  $\delta$  tends to zero.”

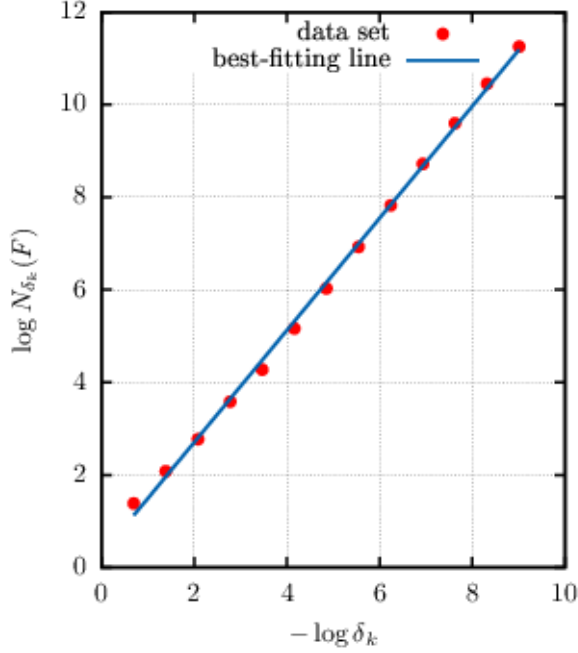


**Figure 20:** Estimation of the box dimension.

**Algorithm.** We approximate the box dimension of a given set  $F$  by estimating the gradient of the graph of  $\log N_\delta(F)$  against  $-\log \delta$ :

1. We first choose a finite sequence of decreasing grid sizes  $\delta_1 > \delta_2 > \dots > \delta_n$ .
2. For all  $\delta_k$ , we compute  $N_{\delta_k}(F)$  and plot  $-\log \delta_k$  against  $\log N_{\delta_k}(F)$ .
3. Finally, we fit the resulting set of data points  $(-\log \delta_k, \log N_{\delta_k}(F))$  with a linear function (e.g., by means of the least squares method) whose slope is the approximation of the box dimension of  $F$ .

Figure 20 shows a plot of the data points and the corresponding best-fitting line for the approximation of the box dimension of the curve segment  $\Lambda_\Theta$  that is illustrated in Figure 19. Here, we use the finite sequence of grid sizes  $\delta_k = 0.5^k$  for  $k = 1, 2, \dots, 13$ . The points  $p, q, r$ , and  $s$  of  $\Theta$  match the vertices of the unit square  $[0, 1] \times [0, 1] \subset \mathbb{R}^2$ , namely  $p = (0, 1)$ ,  $q = (1, 1)$ ,  $r = (1, 0)$ , and  $s = (0, 0)$ ; and the coordinates of the top and bottom point are given by  $(1.0, 0.7)$  and  $(0.0, 0.5)$ . The slope of the fitted line, and thus the approximation of  $\dim_B \Lambda_\Theta$ , is equal to 1.21021.

#### 4.2.2 Setup of the Numerical Experiment

Next, we investigate the box dimension of the curve segment  $\Lambda_\Theta$  as we vary the positions of the top and bottom point of  $\Theta$ . The setup of the numerical experiment

is as follows:

**Initial Marked Box  $\Theta$**  As stated above, let the points  $p$ ,  $q$ ,  $r$ , and  $s$  of the convex marked box  $\Theta$  be given by the vertices of the unit square  $[0, 1] \times [0, 1] \subset \mathbb{R}^2$ . The coordinates of the top and bottom point are given by  $(1, t_2)$  and  $(0, b_2)$  where  $0.1 \leq t_2, b_2 \leq 0.9$ . Theoretically, the marked box  $\Theta$  is convex as long as both parameters are greater than zero and less than one. Yet, we shrink the interval to avoid rounding errors in the computation, which may occur if  $t_2$  or  $b_2$  tend to zero or one.

**Approximation of  $\Lambda_\Theta$**  To compute a finite set of distinguished points of marked boxes that is a subset of the curve segment  $\Lambda_\Theta$ , we modify the iterative scheme from the beginning of this section. If we redefine  $B_0 = \{\Theta\}$  to be the initial set for the iteration and do not change the definition of the sets  $B_j$  for  $j > 0$ , as well as the definition of the sets  $P_j$ , then, for finite  $N \in \mathbb{N}$ , we get

$$\bigcup_{j=0}^N P_j \subset \Lambda_\Theta.$$

Both, the disc space needed to store the set  $\bigcup_{j=0}^N P_j$ , and the time to compute  $P_{j+1}$  given  $P_j$ , grow exponentially in  $N$ . Thus, for all computations, we use  $N = 20$  iterations, which empirically leads to acceptable results in a reasonable amount of time.

**Sequence of Mesh Sizes** We estimate the box dimension of  $\Lambda_\Theta$  using the above-mentioned box-counting algorithm with the finite sequence of grid sizes  $\delta_k = 0.5^k$  for  $k = 1, 2, \dots, 13$ .

### 4.2.3 Results

Using this setup, Figure 21 illustrates the result of the numerical experiment, where the color of each point in the  $[0.1, 0.9] \times [0.1, 0.9]$ -square represents an approximation of the box dimension of  $\Lambda_\Theta$  for different values of the two parameters  $t_2$  and  $b_2$ .

**Symmetric Case** If both parameters are equal to 0.5, then the initial marked box  $\Theta$  is symmetric (see Figure 16), which results in a linear Pappus Curve. The box dimension of the line segment  $\Lambda_\Theta$  is equal to one.

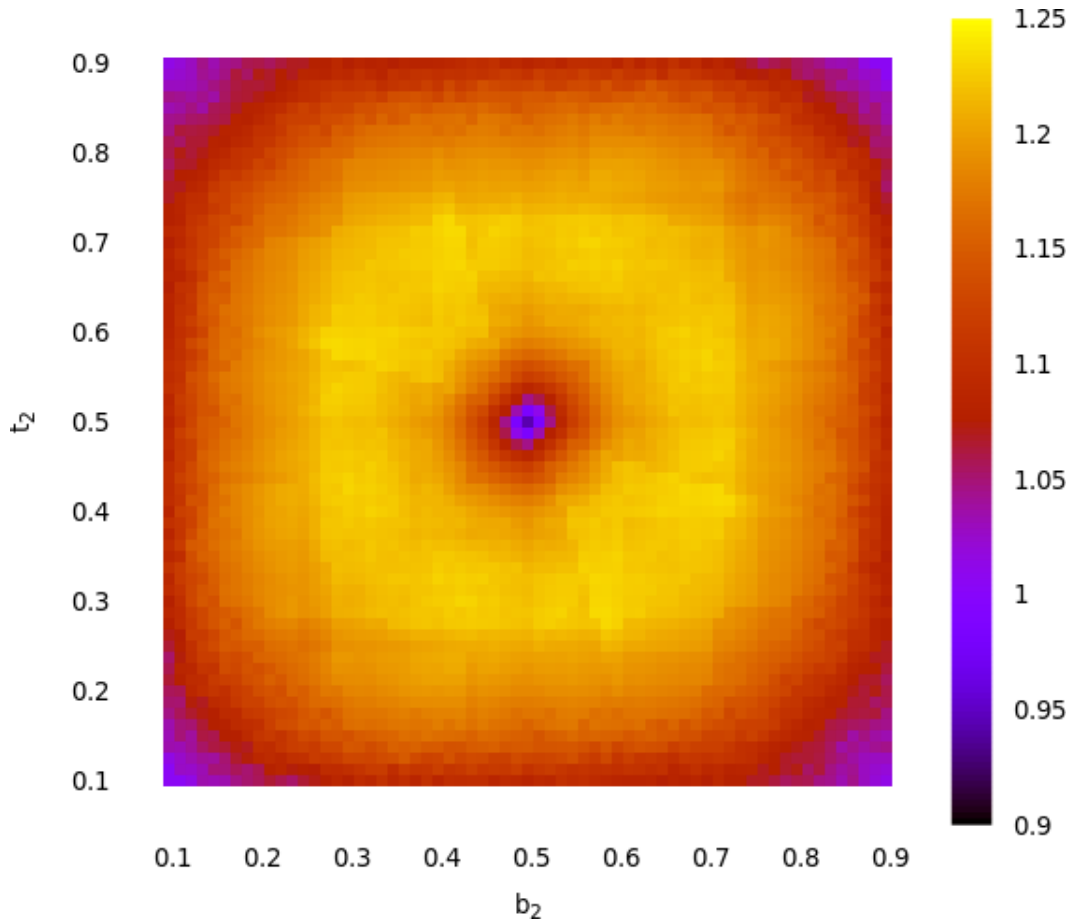


**Figure 21:** Approximation of  $\dim_B \Lambda_\Theta$  for different values of  $t_2$  and  $b_2$ .

**Non-Symmetric Case** If we start in the middle of the  $[0.1, 0.9] \times [0.1, 0.9]$ -square and go towards its boundary on a straight line, we observe that, at first, the box dimension rapidly increases from its minimal value 1.0 to its maximal value 1.25 and then decreases the closer we get to the boundary. The Pappus Curves that are illustrated in the first and second row of Figure 17 show curves whose box dimension is close to the maximum. The box dimension of the third curve in Figure 17 is closer to one, as there are parts of the curve with less sharp edges that resemble segments of straight lines.

## References

- [1] Roger C. Alperin.  $PSL_2(\mathbb{Z}) = Z_2 * Z_3$ . *The American Mathematical Monthly*, 100(4):385–386, 1993.
- [2] Kenneth Falconer. *Fractal Geometry - Mathematical Foundations and Applications*. Wiley, Chichester, 2 edition, 2003.
- [3] Gerd Fischer. *Analytische Geometrie*. Vieweg-Studium; Grundkurs Mathematik. Vieweg, Wiesbaden, 7. edition, 2001.
- [4] Robin Hartshorne. *Foundations of projective geometry*. Lecture notes Harvard University. Benjamin, New York, NY, 1967.
- [5] Tatsuhiko Hatase. *Algebraic Pappus Curves*. Dissertation, Oregon State University, 2011.
- [6] Svetlana Katok. *Fuchsian groups*. Chicago lectures in mathematics series. University of Chicago Press, Chicago, Ill., 1992.
- [7] Richard E. Schwartz. Pappus’s theorem and the modular group. *Publications Mathématiques de l’IHÉS*, 78:187–206, 1993.